AD-769 709

FUEL AND HYDROCARBON VAPORIZATION

BALLISTIC RESEARCH LABORATORIES

AUGUST 1973

AD-769 709

Unclassified
Security Classification

DOCUMENT CONTROL DATA - R & D

(Security classification of title, body of abstract and indexing annotation must be entered when the overall report is classified)

1. ORIGINATING ACTIVITY (Corporate author) USA Ballistic Research Laboratories Aberdeen Proving Ground, Maryland 21005	2a. REPORT SECURITY CLASSIFICATION Unclassified 2b. GROUP

3. REPORT TITLE

Fuel and Hydrocarbon Vaporization

4. DESCRIPTIVE NOTES (Type of report and inclusive dates)

5. AUTHOR(S) (First name, middle initial, last name)

Arthur Gauss

6. REPORT DATE AUGUST 1973	7a. TOTAL NO. OF PAGES 60	7b. NO. OF REFS 16
8a. CONTRACT OR GRANT NO. b. PROJECT NO. 1T1061102A33E c. d.	9a. ORIGINATOR'S REPORT NUMBER(S) BRL REPORT NO. 1661 9b. OTHER REPORT NO(S) (Any other numbers that may be assigned this report)	

10. DISTRIBUTION STATEMENT

Approved for public release; distribution unlimited.

11. SUPPLEMENTARY NOTES	12. SPONSORING MILITARY ACTIVITY U.S.Army Materiel Command Washington, D.C.

13. ABSTRACT

A new semi-empirical expression has been developed which predicts the evaporation rates of pure liquid hydrocarbons under a wide range of conditions. A code has been formulated which, using the above results, calculates the evaporation rates of binary mixtures of hydrocarbons. Extension of these results to real fuels is possible by finding the appropriate binary mixture which approximates the fuel. Analyses of the flammable envelopes surrounding pools of pure hydrocarbon and fuels have also been performed.

DD FORM 1 NOV 68 1473 REPLACES DD FORM 1473, 1 JAN 64, WHICH IS OBSOLETE FOR ARMY USE.

UNCLASSIFIED
Security Classification

14. KEY WORDS	LINK A		LINK B		LINK C	
	ROLE	WT	ROLE	WT	ROLE	WT
Hydrocarbon vaporization, fuel vaporization, liquid pool evaporation, evaporation rate measurements, boundary layer theory analysis of evaporation, evaporation rates from open tubes, one-dimensional diffusion vaporization, three-dimensional diffusion vaporizaton, semi-empirical theory of evaporation, vaporization into air flow, binary mixture evaporation, low pressure vaporization, evaporation of azeatropic mixtures, flammable envelope, lower flammable limit surface, substrate effects on vaporization, heat transfer on vaporization, effects of thickness on evaporation, thermogravimetric analysis of vaporization.						

Destroy this report when it is no longer needed.
Do not return it to the originator.

Secondary distribution of this report by originating or sponsoring activity is prohibited.

Additional copies of this report may be obtained from the National Technical Information Service, U.S. Department of Commerce, Springfield, Virginia 22151.

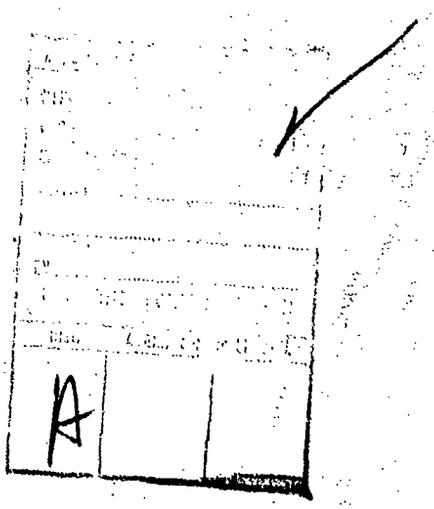

The findings in this report are not to be construed as an official Department of the Army position, unless so designated by other authorized documents.

BALLISTIC RESEARCH LABORATORIES

REPORT NO. 1661

AUGUST 1973

FUEL AND HYDROCARBON VAPORIZATION

A. Gauss

Terminal Ballistics Laboratory

RDT&E Project No. 1T1061102A33E

ABERDEEN PROVING GROUND, MARYLAND

B A L L I S T I C R E S E A R C H L A B O R A T O R I E S

REPORT NO. 1661

AGauss/mba/2040
Aberdeen Proving Ground, Md.
August 1973

FUEL AND HYDROCARBON VAPORIZATION

ABSTRACT

A new semi-empirical expression has been developed which predicts the evaporation rates of pure liquid hydrocarbons under a wide range of conditions. A code has been formulated which, using the above results, calculates the evaporation rates of binary mixtures of hydrocarbons. Extension of these results to real fuels is possible by finding the appropriate binary mixture which approximates the fuel. Analyses of the flammable envelopes surrounding pools of pure hydrocarbons and fuels have also been performed.

TABLE OF CONTENTS

LIST OF ILLUSTRATIONS

LIST OF TABLES

LIST OF SYMBOLS

a		pan radius
c'		mean velocity of gas molecules
c		total molar concentration
c_F		molar concentration of vapor in air
c_{F_o}		molar concentration of vapor at the liquid surface
f	=	$\int \pi_u \, d\eta$, parameter in Blasius equation
k		thermal conductivity
ℓ		depth of liquid below the pan rim
$\dot{m}_v$		mass evaporation rate (gm/sec.)
n		number density in volume V_c
$\dot{n}$		time rate of change of n
n'		number density in region between diaphram and liquid surface nearly equal to n_s
n_o		number density in volume V_c at time zero ($t = o$)
n_s		equilibrium number density, number of molecules per unit volume
n_1		number density in volume V_c at time $t = t_1$
n_{Fo}		mass flux per unit area at the liquid surface
t_1'		time required for number density to reach n_1 with diaphram in place
u_o		average convective air speed in the laboratory room
u_x, u_y		x and y components of air-vapor velocity
u_{yo}		y component of velocity at liquid surface
u_∞		air velocity in + x direction as $y \to +\infty$
v^*		bulk molar velocity
x		distance from leading edge in 2D boundary layer theory
x_F		mole fraction of vapor in air
x_{Fo}		liquid or fuel vapor mole fraction at liquid surface z_o, taken as equilibrium mole fraction

x_{F_1}	liquid or fu vapor mole fraction at z_1
x_1, x_2	liquid mole fractions of liquids 1 and 2
z_o	height of liquid surface in one-dimensional tube
z_1	height of top of one-dimensional tube
A_L	liquid surface area
D	binary diffusion coefficient
$K = \frac{1}{\Lambda_{FA}} \left(\frac{x_{Fo} - x_{F\infty}}{1 - x_{Fo}}\right) \pi'_{FA}(o)$	
K'	a constant here = 1.49, dependent on air velocity distribution
K_H	heat transfer coefficient
L	heat of vaporization
L_c	length of container = V_c/A_L
M	molecular weight
M_F	fuel or liqui molecular weight
N_{Ao}	molar flux of air at the liquid surface = 0
N_{Fo}	molar flux of fuel or pure vapor at the liquid surface
N_{Fz}	evaporation mole flux of fuel or pure vapor at height z
P_A	atmospheric pressure
P_{Fo}	vapor pressure at liquid surface equal to equilibrium vapor pressure
P_{Fo_1} & P_{Fo_2}	vapor pressures of liquids 1 and 2 at their respective surfaces, subscripts 1 and 2 on other parameters in Equation 50 refer to liquids 1 and 2
P_{F1}	vapor pressure at top of 1D tube, $z = z_1$
$\dot{Q}_v$	rate of heat lost in evaporation
R	universal gas constant
Re	Reynolds number = $\frac{2 U_o a}{\nu}$

Sc		Schmidt number = ν/D
T		absolute temperature
T_s		liquid surface temperature
T_{s_1}		surface temperature of liquid 1 with high conductivity base
T_{s_1}'		surface temperature of liquid 1 with low conductivity base
T_A		ambient temperature
T_∞		temperature as $y \to \infty$
V_c		container volume
W_{Fz}		mass flux per unit area
X		ratio x_F/x_{F_0}
z		dimensionless parameter = $z/\sqrt{4Dt}$
α		evaporation coefficient
α_T		thermal diffusivity
β		a constant = 0.34
γ_1		activity coefficient of liquid 1
$\Gamma(1/3, u)$		incomplete gamma function
$\Gamma(1/3, \infty)$		complete gamma function
Δ_u	=	$\nu/\nu = 1$
Δ_T	=	ν/α_T
Δ_{FA}	=	ν/D
μ		viscosity
η		boundary layer parameter defined as = $\frac{y}{2}\sqrt{\frac{u_\infty}{\nu x}}$
ν		kinematic viscosity
θ_u	=	u_x/u_∞, dimensionless velocity
θ_T	=	$T - T_0/T_\infty - T_0$, dimensionless temperature
θ_{FA}	=	$x_F - x_{F_0}/x_{F_\infty} - x_{F_0}$, mole fraction ratio, dimensionless
ρ		mass density of vapor and air
ρ_A		mass density of air

I. INTRODUCTION

A wide range of vaporization problems both experimental and theoretical have been explored. Sections I - V present theoretical analyses of diffusion vaporization, vaporization under uniform flow conditions, and vacuum vaporization. These sections provide the basis for the semi-empirical theoretical models of the more practical problems. Practical experimental results as well as semi-empirical theoretical analyses of these results are presented in Sections VI - X. These sections should be of greatest interest to persons engaged in field tests.

Vaporization even under pseudo-steady state conditions is a complicated phenomena. Vaporization rates for pure liquids are dependent on the air velocity distributions above the liquid, liquid surface temperature, vapor pressure, diffusion coefficient, molecular weight, and geometric factors. A semi-empirical expression has been developed (Section VI) which includes these parameters and which accurately models evaporation from an open pool into a laboratory room where there is slow convective air motion (average speed ~ 3 cm/sec) with velocity fluctuations (see Figure 1). This velocity distribution is closely reproducible over the period of the evaporation rate measurements. Time averaged evaporation rates measured under these conditions are reproducible to better than ± 10%. With slight modification the expression should predict vaporization rates under a wide range of flow conditions not just those mentioned above.

The evaporation rates of simple mixtures are dependent on all of the above pure liquid factors and, in addition, to the liquid phase mole fractions and to the activity coefficients. A simple binary mixture (1/3 pentane - 2/3 octane by volume) has been discovered which simulates the vaporization characteristics of a batch of combat gasoline. A semi-empirical theory (Section VII) which predicts the vaporization rate-time curve for a binary mixture was developed and coded. The code predicts the vaporization rate change with time very accurately for a 1/3 pentane - 2/3 octane mixture (under the same laboratory room

flow conditions described for pure liquids).

In conjunction with evaporation rate analysis the associated problem of concentration profile development around liquid pools was explored both for pure liquids and mixtures (Section VIII). Profiles are determined with a spark probe by locating the flammable volume. Data on steady state and time development of flammable volumes are presented. A limited theory which predicts the height of the flammable volume is suggested.

A graphical analysis of the heat transfer problem associated with an evaporating pure liquid is developed (Section IX). This analysis demonstrates in principle how the liquid evaporation rate may be determined if the surface temperature is unknown. If the surface temperature is unknown then the thermal properties of the air, liquid, and base material as well as the heat of vaporization must be known in addition to all the other properties previously mentioned for pure liquids.

The discussion thus far has been limited to pseudo-steady state conditions. Some one-dimensional time dependent pure diffusion systems are discussed. Also steady state vaporization problems in one, two (with flow), and three-dimensions are discussed. These problems provide a basis for theoretical analysis of the more practical problems.

Although somewhat removed from the rest of the report, a section on vacuum vaporization is included. There is much literature on this subject and it was thought that a section devoted to this topic would help put it in proper perspective.

II. VACUUM VAPORIZATION

Evaporation rates in low pressure vaporization are often less than predicted from kinetic theory by a factor α, the evaporation coefficient. Much attention has been given to determining α and numerous methods have been employed.[1,2,3*] These studies are useful in the design of molecular stills.

**References are listed on page 62.*

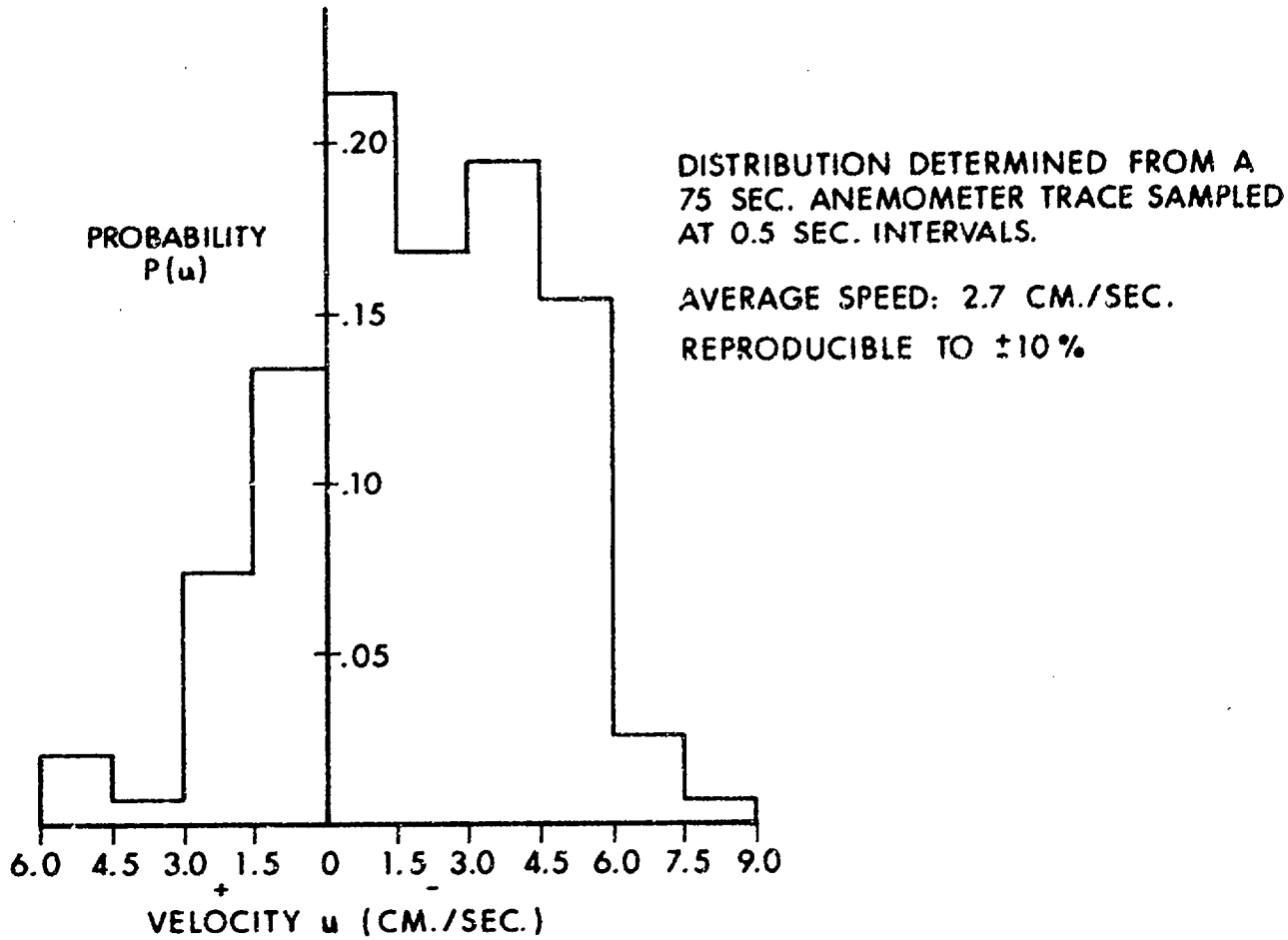

Figure 1. Air Velocity Probability Distribution Along a Line Parallel to the Liquid Surface (TSI 4100 Anemometer).

Let us consider vaporization into a nearly evacuated container of volume V_c from a liquid of surface area A_L. The time development of the number density of molecules (n) in this situation can be written

$$\dot{n} = \frac{A_L}{V_c} \alpha \, c' \, (n_s - n) \tag{1}$$

where

α is the evaporation coefficient

c' is the mean velocity of the gas molecules = $\sqrt{\frac{RT_s}{M \cdot 2\pi}}$

T_s is the liquid surface temperature

M is the liquid molecular weight

R is the universal gas constant

n_s is the equilibrium number density (number of molecules per unit volume at equilibrium).

The above equation is valid only where temperature changes in the liquid can be ignored, a fact which restricts its application to liquids of very low vapor pressure typically glycerol. Integrating the above equation results in

$$\ln \frac{n_s - n_o}{n_s - n_1} = \frac{A_L}{V_c} \alpha \, c' \, t_1 \tag{2}$$

where

n_o is the number density at time zero t = 0

t_1 is the time required for the number density to reach n_1.

Now let us cover the exposed liquid surface with a diaphram which is pierced by a tiny hole of area A_o. The number density in the space between the liquid surface and the diaphram is designated n'. The following equation can be written, similar to Equation (1) for vaporization into V_c

$$\dot{n} = \frac{A_o}{V_c} c' \, (n' - n) \tag{3}$$

integrating this equation results in

$$\ell n \frac{n' - n_o}{n' - n_1} = \frac{A_o}{V_c} c' t_1'. \tag{4}$$

A fairly good assumption is that $n' = n_s$ for very small holes. The time t_1' is the time required for the number density to reach n_1, much longer, of course, than t_1 above. Thus taking the ratio of Equation (2) and Equation (4) the evaporation coefficient is obtained

$$\alpha = \frac{A_o}{A_L} \frac{t_1'}{t_1}. \tag{5}$$

The basic method described above and known as the molecular effusion method has been refined by Heideger and Boudart[2]. The best value of α for glycerol appears to be about 0.05.

It is emphasized here that α appears to be important only in low pressure vaporization. It represents a kind of surface resistance to evaporation.

The maximum rate of vaporization from kinetic theory is given by

$$(\dot{n})_{\text{max th.}} = \frac{c' A_L}{V_c} n_s. \tag{6}$$

The experimental maximum rate is modified by α and is

$$(\dot{n})_{\text{max exp.}} = \alpha \frac{c' A_L}{V_c} n_s. \tag{7}$$

It is interesting to note that Equation (1) can be rewritten

$$\dot{n} = \alpha (L_c c') \left(\frac{n_s - n}{L_c^2}\right) \tag{8}$$

where $L_c = V_c/A_L$ represents a mean free path length.

$\alpha \cdot L_c \cdot c'$ has the dimensions of a diffusion coefficient. Equation (8) then closely resembles the diffusion equation

$$\dot{c}_F = D \frac{\partial^2 c_F}{\partial x^2} \tag{9}$$

but in Equation (8) the effective D ($\alpha \cdot L_c \cdot c'$) is very very large due to the very large mean free path length. c_F in Equation (9) is the vapor concentration. Thus if a liquid is allowed to evaporate into a vacuum, equilibrium will be attained much faster than if it is allowed to evaporate into air.

III. ONE DIMENSIONAL DIFFUSION VAPORIZATION

A. Steady State

The evaporation mole flux (N_{Fz}) for the one dimensional steady state problem with a specified mole fraction (x_{Fo}) at the liquid surface (at height z_o) and another specified mole fraction x_{Fl} (at height z_1) at the top of the tube is

$$N_{Fz} = \frac{cD}{(z_1 - z_o)} \ln \left(\frac{1 - x_{Fl}}{1 - x_{Fo}}\right) \tag{10}$$

where

c is the total molar concentration

D is the binary diffusion coefficient of F in A.

Using vapor pressures instead of mole fractions, the mass flux per unit area is found to be

$$W_{Fz} = \frac{M_F \cdot \frac{P_A}{R \cdot T}}{(z_1 - z_o)} \cdot D \; \ell n \left(\frac{1 - \frac{P_{Fl}}{P_A}}{1 - \frac{P_{Fo}}{P_A}} \right) \quad . \qquad (11)$$

The above theoretical expression has been compared to experiment for 1D open tubes (exposed to a laboratory room) for both cyclohexane and ethyl alcohol. In both cases it is assumed that P_{Fl} is zero, that is, that the air motion in the room is sufficient to maintain a nearly zero concentration at the top of the tube. In addition to comparing the above one dimensional theory with experiment the results are compared with the following mass evaporation rate expression inferred from diffusion vaporization and from 2D boundary layer theory (flow theory). This expression will be discussed in more detail later in this report.

$$\dot{m}_v = \frac{4 \{1 + K'\beta(Re)^{1/2} (Sc)^{1/3}\}}{1 + \frac{4}{\pi} \{1 + K'\beta(Re)^{1/2} (Sc)^{1/3}\} \frac{\ell}{a}} \ell n \left(\frac{1}{1 - \frac{P_{Fo}}{P_A}} \right) \cdot \frac{P_A \cdot M_F}{RT} \cdot D \cdot a \qquad (12)$$

where

$\dot{m}_v$ = total mass evaporation rate

K' = 1.49

β = 0.34

$Re = \frac{2 u_o a}{\nu}$

$Sc = \nu/D$

u_o = average convective air speed in the room (taken to be 3 cm/sec in this case)

ν = kinematic viscosity (μ/ρ)

a = pan radius

D = binary diffusion coefficient

P_{Fo} = vapor pressure at liquid surface

P_A = atmospheric pressure

T = absolute temperature (°K)

M_F = molecular weight

ℓ = depth of liquid below pan rim.

The experimental results obtained here at BRL and the results from the two theories are compared in Table I. All results are for a = 3.7 cm.

Table I. Finite Open Tube Evaporation Rates

LIQUID	ℓ/a	T	$(\frac{gm}{min})$ EXP RATE	$(\frac{gm}{min})$ 1D. THEORY RATE	$(\frac{gm}{min})$ FLOW THEORY RATE
CYCLOHEXANE	0	294°K	.25	∞	.23
	1	297°K	.023	.024	.022
	3	297°K	.0086	.0080	.0077
	5.3	297°K	.0053	.0045	.0045
ETHANOL	0	295°K	.085	∞	.096
	1	296°K	.0110	.0102	.0093
	2	296°K	.0060	.0051	.0049
	3	296°K	.0039	.0034	.0033

One-dimensional open tubes (or Stefan tubes) are one of the primary sources of gas phase diffusion coefficients. Mass evaporation rates from the tube are measured and the one-dimensional theory is used to calculate the diffusion coefficient (D). A carefully controlled flow of air (or other carrier gas) is passed over the mouth of the tubes to insure zero concentration at the top. Such methods have been used recently by Lee and Wilke[4] (1954) and by Altshuller and Cohen[5] (1960) to determine diffusion coefficients. The concentration profiles in a Stefan tube have been investigated experimentally by Heinzelmann, Wason, and Wilke[6] (1965) and have been found to agree well with the theory.

B. Time Dependent Infinite Open Tube

Exact solutions exist for the one-dimensional time dependent system of infinite length. Discussion of this specific evaporation problem is presented by Bird, Stewart and Lightfoot[7] and for a general class of problems of this type by Danckwerts[8].

In the discussion in Bird the liquid surface is kept at a fixed level ($z = 0$) and it is assumed that the flux of air at this point is zero $N_{Ao} = 0$. The following species equation is solved

$$\frac{\partial x_F}{\partial t} = D \frac{\partial^2 x_F}{\partial z^2} + \frac{D}{1 - x_{Fo}} \frac{\partial x_F}{\partial z} \bigg|_{z = 0} \frac{\partial x_F}{\partial z} \tag{13}$$

subject to the following boundary and initial conditions

$$x_F = 0 \qquad t = 0$$

$$x_F = x_{Fo} \qquad z = 0$$

$$x_F = 0 \qquad z \to \infty \, .$$

The above equation is converted to dimensionless form and the solution is

$$X = \frac{1 - \text{erf}\,(Z - \phi)}{1 + \text{erf}\,\phi} \tag{14}$$

where

$$X = x_F / x_{Fo}$$

$$Z = \frac{z}{\sqrt{4\,Dt}}$$

$$\phi = -\frac{1}{2} \frac{x_{Fo}}{1 - x_{Fo}} \frac{dX}{dZ} \bigg|_{z = 0}.$$

A knowledge of x_{Fo} is sufficient to determine ϕ from

$$x_{Fo} = \frac{1}{1 + [\sqrt{\pi}\ (1 + \text{erf}\ \phi)\ \phi\ \exp\ \phi^2]^{-1}} \qquad (15)$$

ϕ may be thought of as a dimensionless bulk velocity, in fact the bulk molar velocity (v*) is related to ϕ by

$$v^* = \phi\ \sqrt{D/t}$$

v* is zero only for $x_{Fo} = 0$. v* is known as the Stefan flow[9]. There can be no diffusion vaporization without some convection v*. The solution X for various values of x_{Fo} is shown in Figure 2.

The rate of evaporation (volume rate) is given by

$$\frac{d\ V_F}{dt} = A\ \phi\ \sqrt{D/t} \qquad (16)$$

where A is the cross sectional area of the tube. Relations of the above type have been known for many years, in fact a verification of it was presented by M. P. Vaillant in 1910[10] (Vaillant uses the Fick's second law approximation, ϕ small and $\phi = \frac{x_{Fo}}{\sqrt{\pi}}$ in equation (16)).

It is of interest to note that the time dependent finite open tube problem with zero concentration at the top and fixed concentration at the liquid surface (initial assumption of zero vapor concentration in the tube) has an analytical solution in terms of Fourier series. The results for the analogous heat flow problem are presented by Tarifa[11].

C. <u>One-Dimensional Closed System</u>

In connection with the problem of concentration profiles in a fuel tank a one-dimensional time dependent analysis of a closed system was performed. The initial conditions are that no fuel vapor is initially

$$X = \frac{X_F}{X_{F_o}} \qquad Z = \frac{z}{\sqrt{4Dt}}$$

$$X = \frac{1 - \text{erf}\,(Z - \phi)}{1 + \text{erf}\,\phi}$$

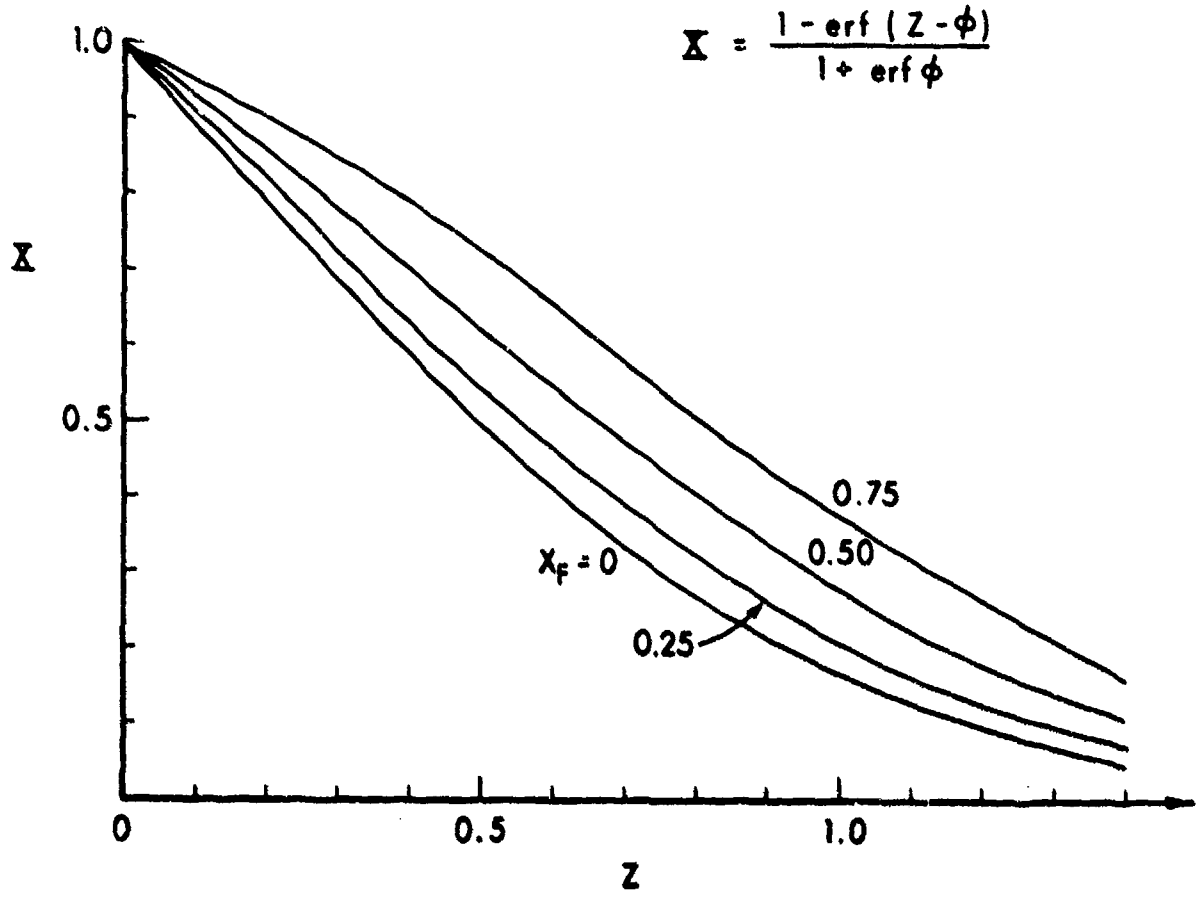

Figure 2. Concentration Profiles, Infinite Open Tube.

present in the region above the fuel surface. Boundary conditions are that a fixed concentration exists at the liquid surface (c_{Fo}) and that the flux of fuel at the top of the tank is zero, $D \left(\frac{\partial c_F}{\partial z}\right)_{z = L_c} = 0$.

The equation to be solved is

$$\frac{\partial c_F}{\partial t} = D \frac{\partial^2 c_F}{\partial z^2} \tag{17}$$

subject to the above mentioned conditions. The solution to this equation is obtained by a standard separation of variables method and a Fourier series expansion of the concentration. The result is

$$c_F(z, t) = c_{Fo} \left(1 - \sum_{n = 1,3,5,7 \ldots} \frac{4}{n\pi} \sin \frac{n\pi z}{2L_c} e^{-\frac{n^2\pi^2}{(2L_c)^2} Dt} \right). \tag{18}$$

It is important to note that the above result is only valid for small fuel concentration at the surface (certainly no greater than twenty percent by mole fraction).

An approximation to the pressure as a function of time in this closed system can be obtained by integrating the above expression for the concentration. The result is

$$P = P_A + P_{Fo} \left(1 - \sum_{n = 1,3,5,7 \ldots} \frac{8}{\pi^2 n^2} e^{-\frac{n^2\pi^2}{(2L_c)^2} Dt} \right) \tag{19}$$

where

P_A is atmospheric pressure

P_{Fo} is the vapor pressure of the hydrocarbon fuel.

The concentration profiles as a function of time and the pressure-time relationship are shown in Figures 3 and 4.

IV. TWO DIMENSIONAL VAPORIZATION INTO FLOW

The following equations are considered in this analysis of the flow problem where the liquid surface is considered flat and rigid, (Figure 5).

$$\frac{\partial u_x}{\partial x} + \frac{\partial u_y}{\partial y} = 0 \qquad \text{continuity}$$

$$u_x \frac{\partial u_x}{\partial x} + u_y \frac{\partial u_x}{\partial y} = \nu \frac{\partial^2 u_x}{\partial y^2} \qquad \text{momentum}$$

$$u_x \frac{\partial T}{\partial x} + u_y \frac{\partial T}{\partial y} = \alpha_T \frac{\partial^2 T}{\partial y^2} \qquad \text{energy} \qquad (20)$$

$$u_x \frac{\partial x_F}{\partial x} + u_y \frac{\partial x_F}{\partial y} = D \frac{\partial^2 x_F}{\partial y^2} \qquad \text{species F}$$

with the following boundary conditions

for

$$x \leq 0 \text{ or } y \to \infty: u_x = u_\infty, T = T_\infty, x_F = x_{F\infty}$$

at

$$\left.\begin{matrix} y = 0 \\ x > 0 \end{matrix}\right) : u_x = 0, T = T_0, x_F = x_{Fo}, N_{Ao} = 0.$$

$$C_F(z,t) = C_{F_o}\left(1 - \sum_{n=1,3,5,7\ldots} \frac{4}{n\pi} \sin\frac{n\pi z}{(2L_c)} e^{-\frac{n^2\pi^2}{(2L_c)^2} Dt}\right)$$

L_c = 15 CM.

D = 0.10 CM.^{2}/ SEC.

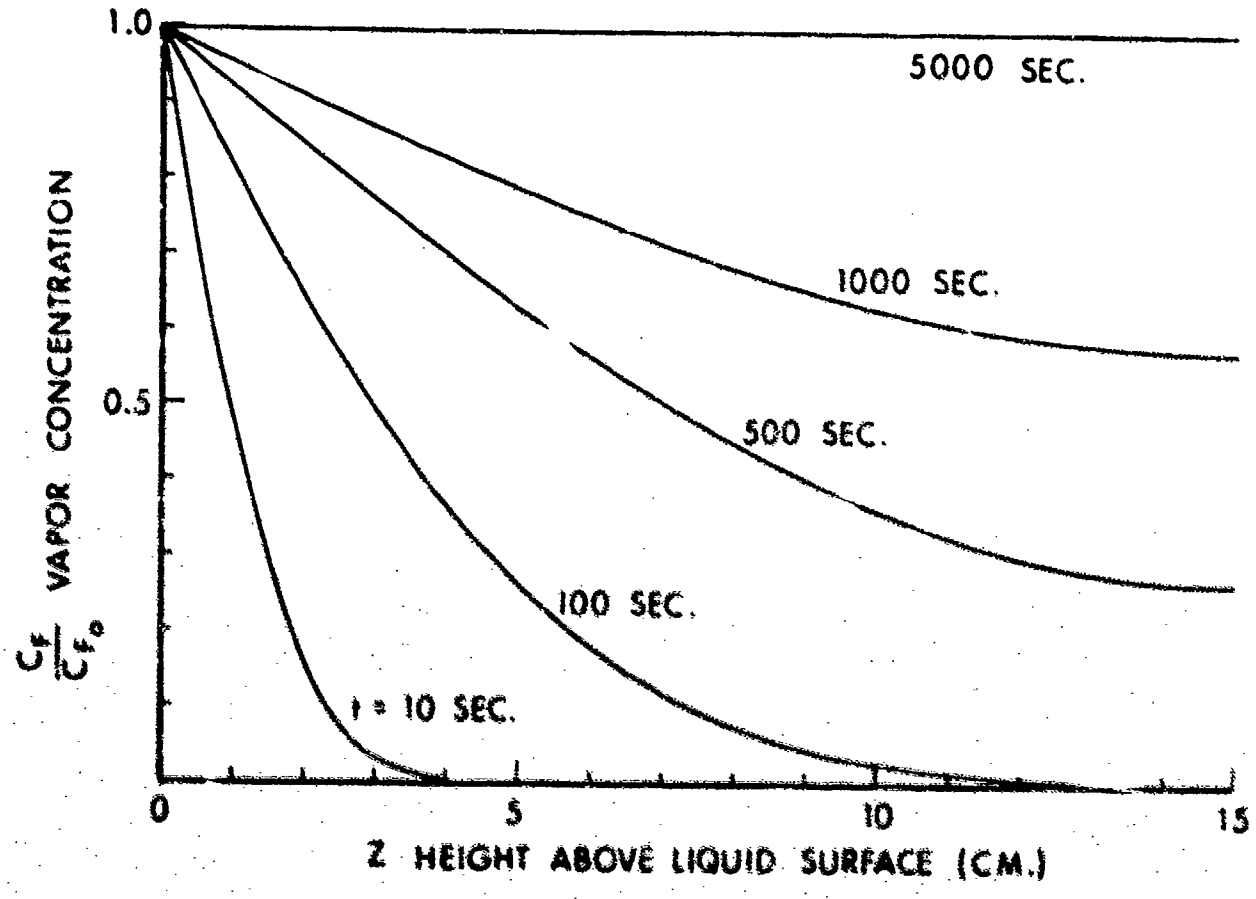

Figure 3. Concentration Profiles in Closed Fuel Tank.

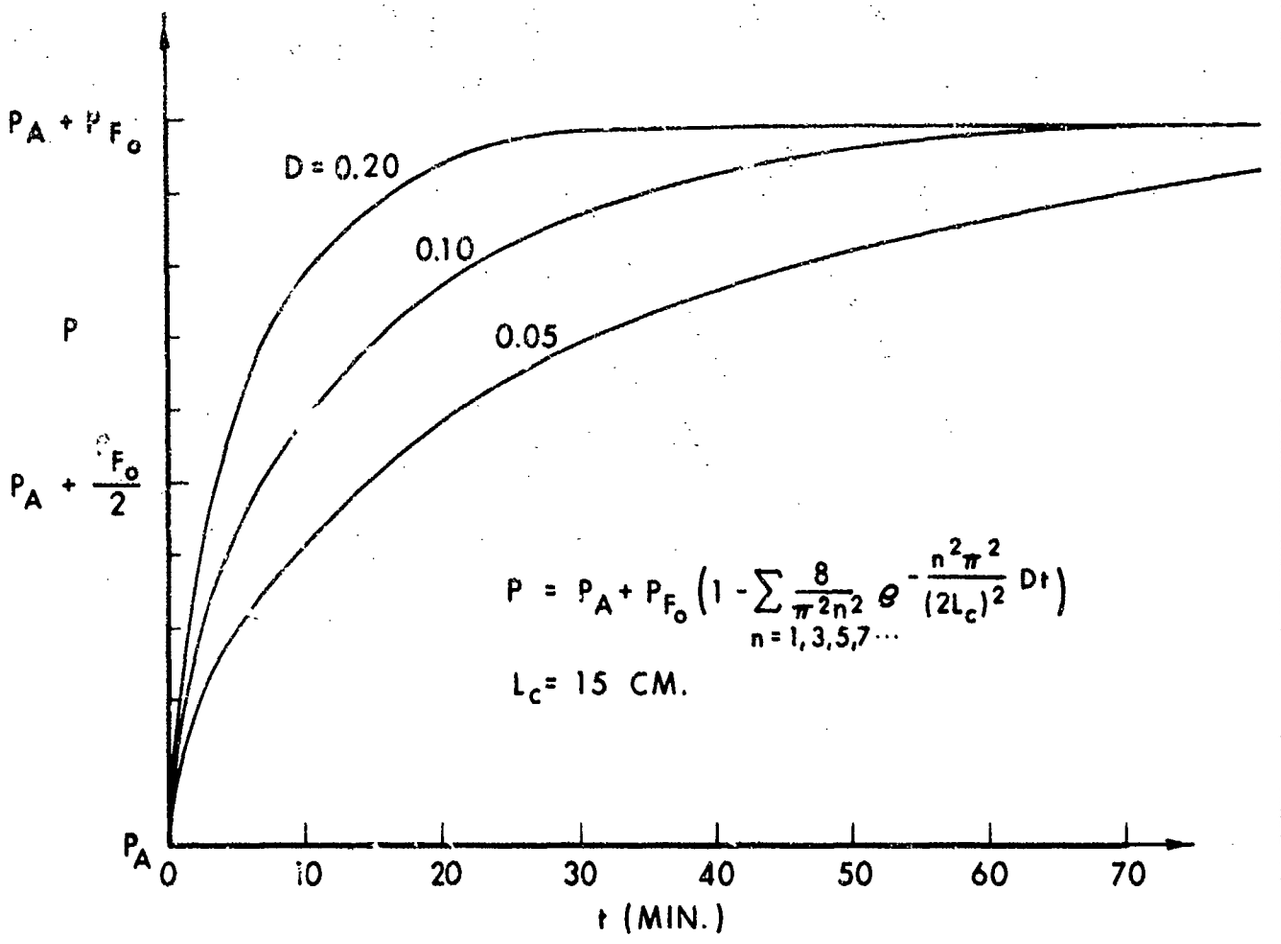

Figure 4. Pressure in Closed Fuel Tank.

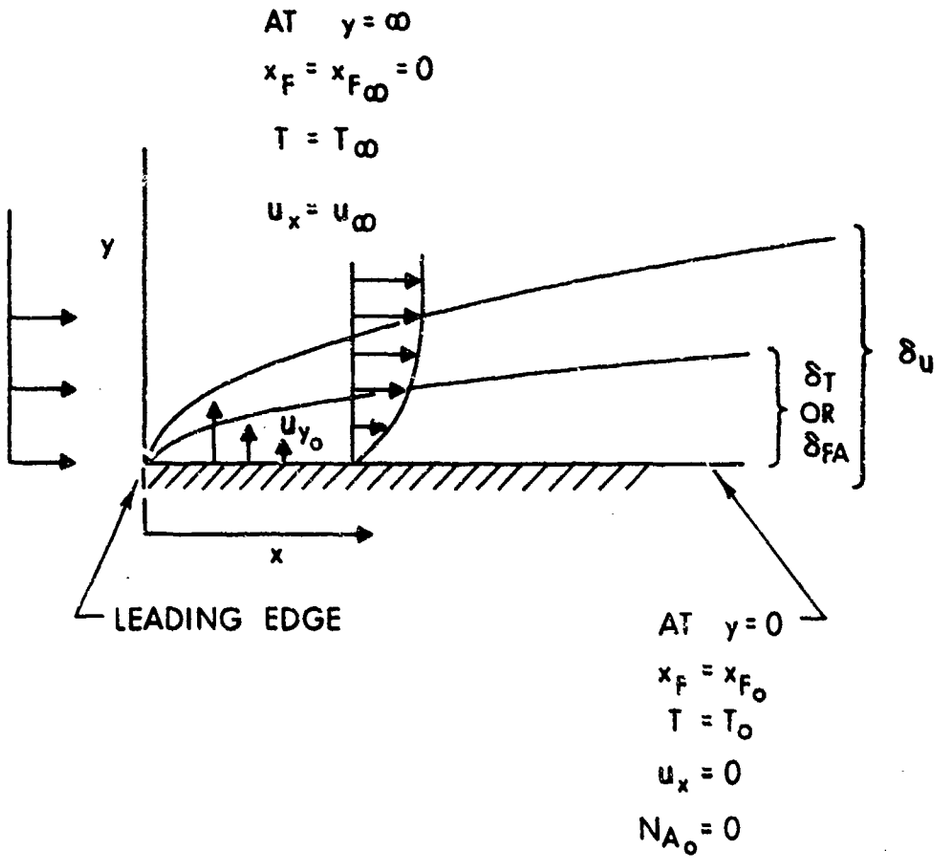

Figure 5. Two-Dimensional Vaporization with Flow.

No chemical reactions are assumed here and species A represents ambient air into which species F is evaporating. The following properties are assumed constant ρ, u, C_p, k, c and D. First the continuity equation is solved for u_y

$$u_y = u_{yo} - \int_o^y \frac{\partial u_x}{\partial x}\, dy \tag{21}$$

or in terms of the molar flux of F at the surface (N_{Fo})

$$u_y = \frac{M_F N_{Fo}}{\rho} - \int_o^y \frac{\partial u_x}{\partial x}\, dy. \tag{22}$$

Fick's first law gives

$$N_{Fo} = - c\, D \left.\frac{\partial x_F}{\partial y}\right|_{y=0} + x_{Fo}\,(N_{Fo} + N_{Ao}) \tag{23}$$

but $N_{Ao} = 0$, thus substituting for N_{Fo} into equation (22) above the result is

$$u_y = - \frac{M_F}{\rho}\, c \cdot \frac{D}{(1 - x_{Fo})} \left.\frac{\partial x_F}{\partial y}\right|_{y=0} - \int_o^y \frac{\partial u_x}{\partial x}\, dy\ . \tag{24}$$

but the original assumption ρ = const., c = const., force $M_A = M_F$ and thus $\frac{M_F \cdot c}{\rho} = 1$. Therefore,

$$u_y = - \frac{D}{(1 - x_{Fo})} \left.\frac{\partial x_F}{\partial y}\right|_{y=0} - \int_o^y \frac{\partial u_x}{\partial x}\, dy\ . \tag{25}$$

u_y is substituted into the momentum, energy, and species equations to obtain the following common form for the three equations

$$\Lambda \left\{ \frac{1}{\Lambda_{FA}} \left(\frac{x_{Fo} - x_{F\infty}}{1 - x_{Fo}} \right) \pi'_{FA}(o) - \int_o^\eta 2\pi_u \, d\eta \right\} \pi' = \pi'' \qquad (26)$$

or (defining K)

$$- \Lambda \left\{ - K + \int_o^\eta 2\pi_u \, d\eta \right\} \pi' = \pi'' \qquad (27)$$

where π may be

$$\pi_u = \frac{u_x}{u_\infty}, \; \pi_T = \frac{T - T_o}{T_\infty - T_o} \; ; \; \pi_{FA} = \frac{x_F - x_{Fo}}{x_{F\infty} - x_{Fo}}$$

and Λ may be

$$\Lambda_u = \frac{\nu}{\nu} = 1, \; \Lambda_T = \frac{\nu}{\alpha} \Lambda_{FA} = \frac{\nu}{D}$$

and the prime denotes differentiation with respect to

$$\eta = \frac{y}{2} \sqrt{\frac{u_\infty}{\nu x}} \; .$$

The boundary conditions are

$$\eta = 0, \; \pi = 0; \; \eta \to \infty, \; \pi \to 1.$$

Analytical sclutions are obtainable in the 2D case only for small K and moderate to large values of Λ_{FA}.

An interesting point can be made at this juncture. Consider the general equation written for the momentum case

$$- \Lambda_u \{ - K + \int_o^\eta 2 \, \pi_u \, d\eta \} \, \pi'_u = \pi''_u. \qquad (28)$$

Now with K = 0 (no evaporation or condensation) the above becomes

$$- \{ \int_o^\eta 2 \, \pi_u \, d\eta \} \, \pi'_u = \pi''_u; \; \Lambda_u = 1. \qquad (29)$$

Now letting $\pi_u = \frac{\partial f}{\partial \eta}$ the above is

$$- 2f \frac{\partial^2 f}{\partial \eta^2} = \frac{\partial^3 f}{\partial \eta^3} \tag{30}$$

which is just the Blasius equation[12] and has a well known solution.

To obtain the evaporation mass flux the species version of equation (26) above is solved giving (for small K)

$$\pi_{FA} (\eta, \Lambda_{FA}, K) = \frac{\Gamma (1/3, u)}{\Gamma (1/3, \infty)} \tag{31}$$

where

$$u = 1.328 \frac{\Lambda_{FA} \eta^3}{3} . \tag{32}$$

The derivative at the liquid surface is (for small K)

$$\pi'_{FA} (0, \Lambda_{FA}, K) = 0.68 \Lambda_{FA}^{1/3}. \tag{33}$$

Now using the definition of K and assuming $x_{F\infty} = 0$ the result is

$$K = \frac{1}{\Lambda_{FA}} \cdot \frac{x_{Fo}}{1 - x_{Fo}} \cdot \pi'_{FA} (0). \tag{34}$$

Substituting for $\pi'_{FA} (0)$ and assuming x_{Fo} small, the above becomes

$$K = \frac{x_{Fo}}{\Lambda_{FA}^{2/3}} 0.68. \tag{35}$$

Fick's first law gives

$$K = 2\, n_{Fo} \sqrt{\frac{x}{u_\infty \mu \rho}} \tag{36}$$

n_{Fo} is the mass flux per unit area of fuel at the surface. Solving for n_{Fo}, the following interesting result is obtained

$$n_{Fo} = 0.34 \cdot \left(\frac{D}{\nu}\right)^{2/3} \cdot x_{Fo} \cdot \sqrt{\frac{u_\infty \cdot \mu \cdot \rho}{x}} \,. \tag{37}$$

The above result was obtained assuming $M_F = M_A$. Experiment, however, indicates it is valid even for $M_F \neq M_A$. Including the molecular weight factor (M_F/M_A) the result is

$$n_{Fo} = 0.34 \left(\frac{D}{\nu}\right)^{2/3} \cdot \left(\frac{M_F}{M_A}\right) \cdot \frac{P_{Fo}}{P_A} \cdot \sqrt{\frac{u_\infty \cdot \mu \cdot \rho}{x}} \tag{38}$$

where $P_{Fo}/P_A = x_{Fo}$ and P_{Fo} is the fuel (liquid) vapor pressure at the surface, P_A is atmospheric pressure.

The above expression for n_{Fo} can be integrated over a surface area to give the total mass evaporated per unit time for the area into a unidirectional flow parallel to the surface.

To integrate n_{Fo} over a circular liquid surface the surface is considered to be made up of a series of rectangles with long sides parallel to the flow. The two dimensional model above is applied to each rectangle assuming no interaction between rectangles. The following diagram illustrates the method of integration.

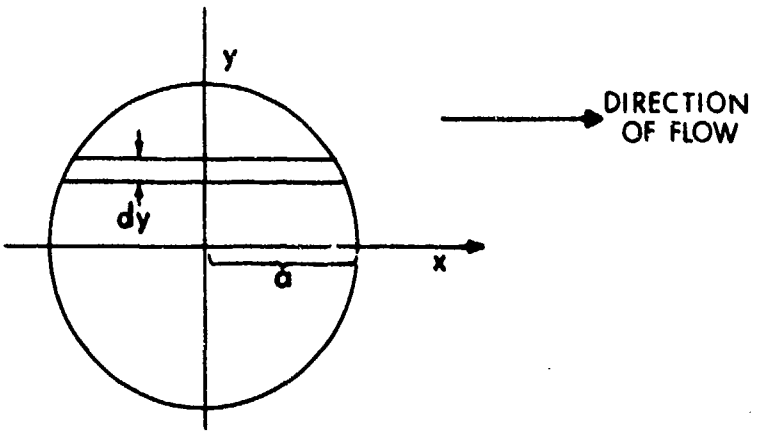

The total mass evaporated per unit time from a rectangle of width 'dy' is

$$\dot{m}_V\,(dy) = 0.34\,\left(\frac{D}{\upsilon}\right)^{2/3} \cdot \frac{P_{Fo}}{P_A} \cdot (u_\infty \cdot \mu \cdot \rho)^{1/2} \cdot \frac{M_F}{M_A} \cdot \left\{ \int_{-\sqrt{a^2 - y^2}}^{+\sqrt{a^2 - y^2}} \frac{dx}{(x + (a^2 - y^2)^{1/2})^{1/2}} \right\} dy. \qquad (39)$$

Integrating over 'x' results in

$$\dot{m}_V\,(dy) = 0.34\,\left(\frac{D}{\upsilon}\right)^{2/3} \cdot \frac{P_{Fo}}{P_A} \cdot (u_\infty \cdot \mu \cdot \rho)^{1/2}\; 2\sqrt{2}\;(a^2 - y^2)^{1/4} \frac{M_F}{M_A}\, dy. \qquad (40)$$

The total rate is obtained by integrating over y from -a to +a. The integral is obtained using Simpson's rule on a 9810A H.P. calculator. The result is

$$\dot{m}_V = 0.34\,\left(\frac{D}{\upsilon}\right)^{2/3} \cdot \frac{P_{Fo}}{P_A} \cdot \frac{M_F}{M_A}\,(u_\infty \cdot \mu \cdot \rho)^{1/2} \cdot 4\sqrt{2} \cdot 0.863 \cdot a^{3/2} \qquad (41)$$

or written in terms of the Reynold's number and the Schmidt number

$$\dot{m}_V = 0.34 \cdot \frac{P_{Fo}}{P_A} \cdot \frac{M_F}{M_A} \cdot (Sc)^{1/3} \cdot (Re)^{1/2} \cdot \rho \cdot a \cdot 3.45 \cdot D \qquad (42)$$

for evaporation from a circular fluid surface into a uniform stream of air parallel to the surface, where

$$Sc = \frac{\nu}{D} \qquad Re = \frac{2\, u_\infty\, a}{\nu}$$

ρ is the density of air and vapor nearly equal to ρ_A (air density) for small vapor pressures. A square with side length '2a' would give a closely similar result, 3.45 would be replaced by 4.00.

A result showing a like dependence on the Schmidt and Reynolds numbers for evaporation from a planar surface has been obtained by other investigators[13].

V. THREE DIMENSIONAL DIFFUSION VAPORIZATION

One problem of interest is evaporation from an open pan into a perfectly still atmosphere. In such a situation diffusion of vapor into the air controls the evaporation. In its simplest form (assumption that the vapor pressure is small compared to atmospheric pressure) the problem reduces to the solution of Laplace's equation for the concentration in three dimensions subject to the following boundary conditions: zero concentration at infinity, zero vapor flux from r = a (pan radius) to infinity in the plane of the pan, and equilibrium vapor concentration at the liquid surface. These boundary conditions are summarized in Figure 6. The solution curves of equal concentration are ellipsoids centered on the pan and are shown in Figure 7. The solution along the z axis has a simple form and is given by

$$c_F = \frac{2\, c_{Fo}}{\pi} \tan^{-1} \frac{a}{z} . \qquad (43)$$

Likewise the solution in the plane of the pan has a simple form

$$c_F = \frac{2\, c_{Fo}}{\pi} \sin^{-1} \frac{a}{r} . \qquad (44)$$

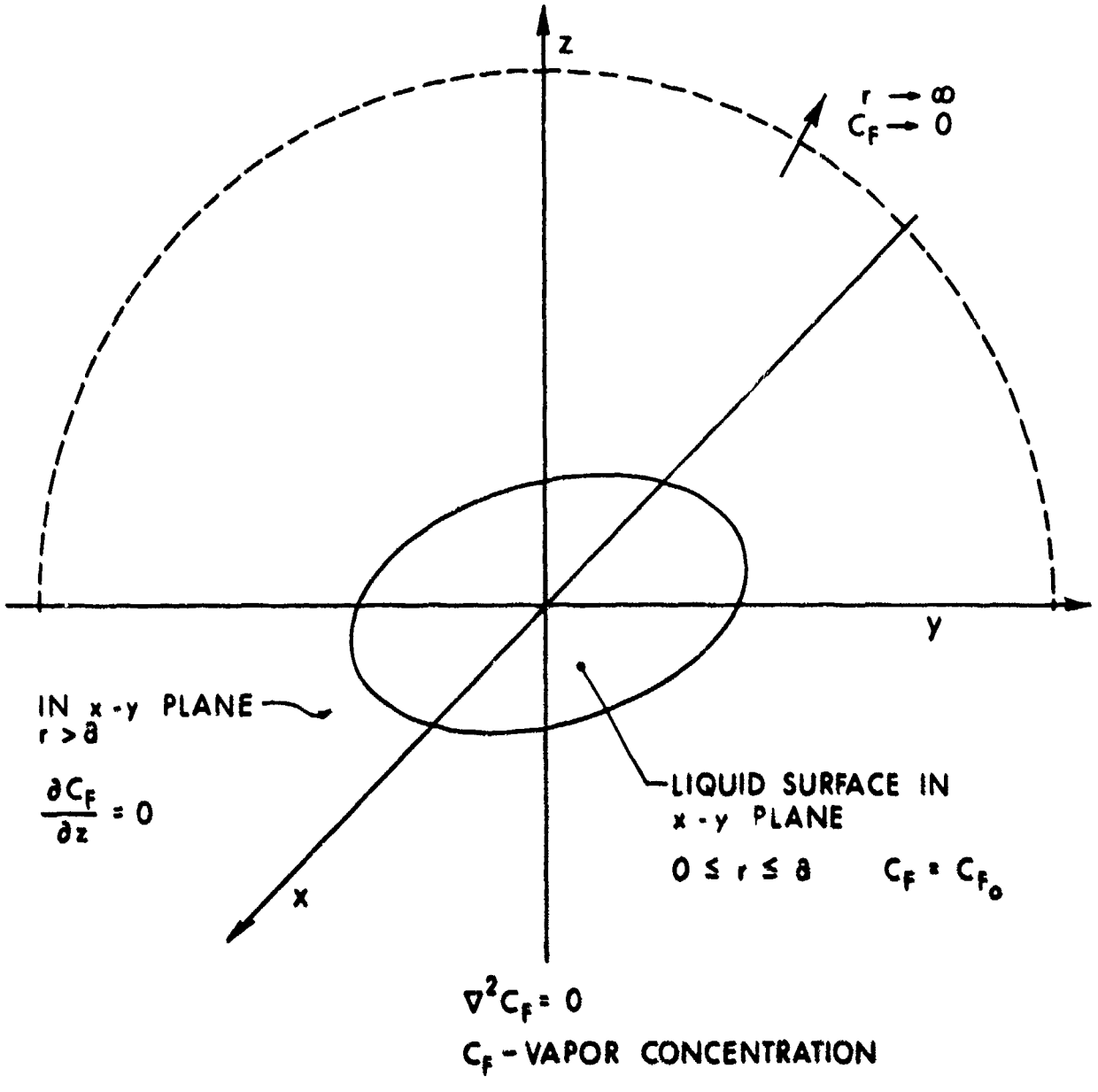

Figure 6. Boundary Conditions, Three-Dimensional Laplace Equation.

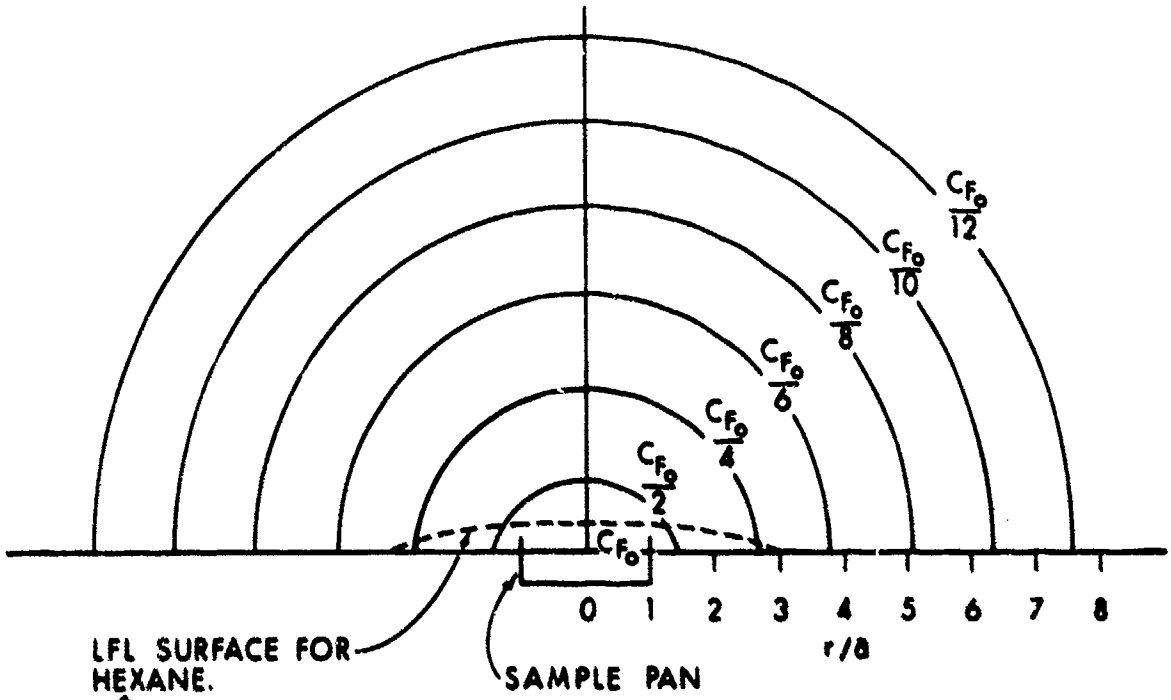

Figure 7. Solution to the Three-Dimensional Laplace Equation.

For moderate to large values of r/a the equi-concentration profiles are very nearly spherical. The mass evaporation rate from a pan of radius 'a' according to this theory is

$$\dot{m}_v = 4 \cdot D \cdot \frac{M_F}{M_A} \cdot \frac{P_{Fo}}{P_A} \cdot a \cdot \rho_A \tag{45}$$

where all the symbols have been defined previously.

The above solution is based on the assumption of small surface concentration (small P_{Fo}/P_A). The evaporation rate expression extended to large values of P_{Fo}/P_A is

$$\dot{m}_v = 4 \cdot D \cdot \frac{M_F}{M_A} \cdot \left(\ln \frac{1}{1 - \frac{P_{Fo}}{P_A}}\right) \cdot a \cdot \rho_A$$

$$= 4 \cdot D \cdot \frac{M_F P_A}{RT} \cdot a \cdot \left(\ln \frac{1}{1 - \frac{P_{Fo}}{P_A}}\right) . \tag{46}$$

The above result is due originally to Stefan as reported by Thomas and Ferguson[14] and of course reduces to the previous result for small P_{Fo}/P_A.

VI. COMBINED MASS EVAPORATION RATE EXPRESSION

The combined mass evaporation rate expression was formulated to fit the data of a laboratory experiment which simulates real world conditions. The experiment consists of a liquid in a circular pan which is allowed to evaporate into a room where there is a slow air flow of some 3 cm/sec. passing over the pan (average velocity component in the direction of flow). The fluctuations in the air flow both parallel and transverse to the flow direction are some ± 5 cm/sec. These fluctuations lead, of course, to reversals in the flow direction at times. DISA (DISA Electronics, Franklin Lakes, N.J.) and TSI (Thermo-Systems Inc., Saint Paul,

Minn.) low velocity anemometers were employed for the flow measurements. The flow velocity distribution (see Figure 1) is quite reproducible over the period of the evaporation rate measurements. The experimental evaporation rates (time averaged over a few minutes) are reproducible to within ± 10% (nearly steady state thermal conditions must be attained indicated by nearly steady liquid surface temperature before measurements are made).

The theoretical results of the previous two sections (diffusion into air flow and pure diffusion) can be combined together into a single equation for the mass evaporation rate. The result is (assuming a unidirectional flow over the pan and small surface concentration of fuel vapor)

$$\dot{m}_v = 4 \{1 + 0.863 \beta (Re)^{1/2} (Sc)^{1/3}\} \left(\frac{P_{Fo}}{P_A}\right) \cdot \frac{P_A}{RT} \cdot M_F \cdot D \cdot a \,. \qquad (47)$$

An equation of similar form showing the same dependence on Reynolds number and Schmidt number (due to Frössling as reported by Fuchs[9]) has been used for years to successfully describe droplet evaporation even at very low Reynolds number (≤ 10) where there is no current theory. It is very important to note that the component of vaporization in the above equation due to flow is greater than the pure diffusion component even at flows of 1 cm/sec (for the range of pan radii considered). Thus, even very small flows significantly effect the evaporation rate.

The above theoretical Frössling equation is valid for unidirectional flow. The actual experiment which is to be described does have a small unidirectional flow component, however, there are large fluctuations about this velocity. It would appear to be important to obtain velocity probability distributions along three mutually orthogonal axes. These distributions should completely characterize the flow. External flow is very important in the actual experiment. The flow characteristics and hence the evaporation rate can be changed by opening and closing air conditioning ducts in the laboratory room.

In an attempt to simply describe evaporation into the laboratory room (without using probability distributions) a Frössling like equation was adopted. The mean measured air speed (direction not considered) over the liquid surface was used in the Reynolds number (~ 3 cm/sec). The equation has the form

$$\dot{m}_v = 4 \{1 + K' B (Re)^{1/2} (Sc)^{1/3}\} \ln \left(\frac{1}{1 - \frac{P_{Fo}}{P_A}}\right) \cdot \frac{P_A}{RT} \cdot M_F \cdot D \cdot a \quad (48)$$

where K' is a constant dependent on the pan geometry and the flow velocity distribution (K' is determined by fitting the data for one liquid, in this case cyclohexane). $\frac{P_{Fo}}{P_A}$ is replaced by $\ln \left(\frac{1}{1 - \frac{P_{Fo}}{P_A}}\right)$ in the hope of extending agreement to higher vapor pressures.

The worst deviation between theory and experiment is 30% with other rates in much better agreement. The expression fits the data well (see Table II to compare theory and experiment).

The question of the effect of relative humidity on evaporation rates has not been addressed. Relative humidity does not appear to be significant for all the liquids tested except, of course, for water. The range of humidity encountered in these experiments is from 45 to 60 per cent.

For $\ell/a \neq 0$ (ℓ is the depth of the liquid below the pan rim) the Frössling equation above has been further modified. The modified equation is as follows

$$\dot{m}_v = \frac{4 \{1 + K' B (Re)^{1/2} (Sc)^{1/3}\}}{1 + \frac{4}{\pi} \{1 + K' B (Re)^{1/2} (Sc)^{1/3}\} \frac{\ell}{a}} \ln \left(\frac{1}{1 - \frac{P_{Fo}}{P_A}}\right) \cdot \frac{P_A}{RT} \cdot M_F \cdot D \cdot a. \quad (49)$$

For very large ℓ/a the above reduces to the one-dimensional theoretical result for evaporation from an open tube with zero concentration at the

TABLE II

EVAPORATION RATE DATA $\Delta/\theta = 0$ (GM./MIN.)

PAN DIAMETER	2.40 CM.			7.40 CM.			12.5 CM.			17.6 CM.		
	T	TH	E	T	TH	E	T	TH	E	T	TH	E
TEST LIQUIDS												
ACETONE	293	.108	.086	288	0.40	0.37	284	0.73	0.69	281	1.01	1.07
HEXANE	296	.083	.080	291	0.33	0.36	288	0.61	0.72	287	0.97	1.12
CYCLOHEXANE	295	.049	.045	294	0.23	0.25	293	0.465	0.50	291	0.71	0.82
ETHANOL	298	.0225	.020	295	0.096	0.085	294	0.195	0.18	294	0.32	0.31
OCTANE	300	.0101	.0090	299	0.050	0.056	298	0.101	0.103	297	0.155	0.170
BUTANOL	299	.0041	.0031	298	0.019	0.016	298	0.041	0.036	298	0.067	0.056
WATER	300	.0026	.0022	296	0.012	0.012	299	0.026	0.023	298	0. 39	0.032
DECANE	300	.0014	.0010	299	0.0071	0.0055	299	0.015	0.012	300	0.026	0.021

T - SURFACE TEMPERATURE °K
TH - THEORY RESULTS
E - EXPERIMENTAL RESULTS

top. The flow in the room maintains approximately zero concentration at the end of the tube for large ℓ/a. The above equation, as mentioned in Section IIIA, was applied to cyclohexane and ethanol for $\ell/a \neq 0$. (See also Figure 8).

The combined rate expression has been shown to be effective in analyzing the experiments conducted thus far. The expression contains terms which are characteristic of mass transfer in flow systems (Reynolds number and Schmidt number). The flow term ($K' \, Re^{1/2} \, Sc^{1/3}$) is dominant over all the pan sizes considered here. However, by going to very small pans (~ 1/2 cm. rad. or less) the pure diffusion term would dominate. The average evaporation rate per unit area increases tremendously as one goes to very small pans and the average velocity of the vapor leaving the liquid surface eventually becomes large compared to the background convective air speed in the room. Terms accounting for vapor density variations have not been included and do not appear to be important for predicting the evaporation rate under the conditions considered here.

For moderate values of the convective air speed the combined rate expression predicts a nearly $a^{3/2}$ dependence of the evaporation rate for a particular liquid ($\frac{\ell}{a} = 0$). This is in close agreement with experimental results obtained years ago by Ferguson and Thomas[14] for water evaporating into a laboratory room ($\ell/a \approx 0$).

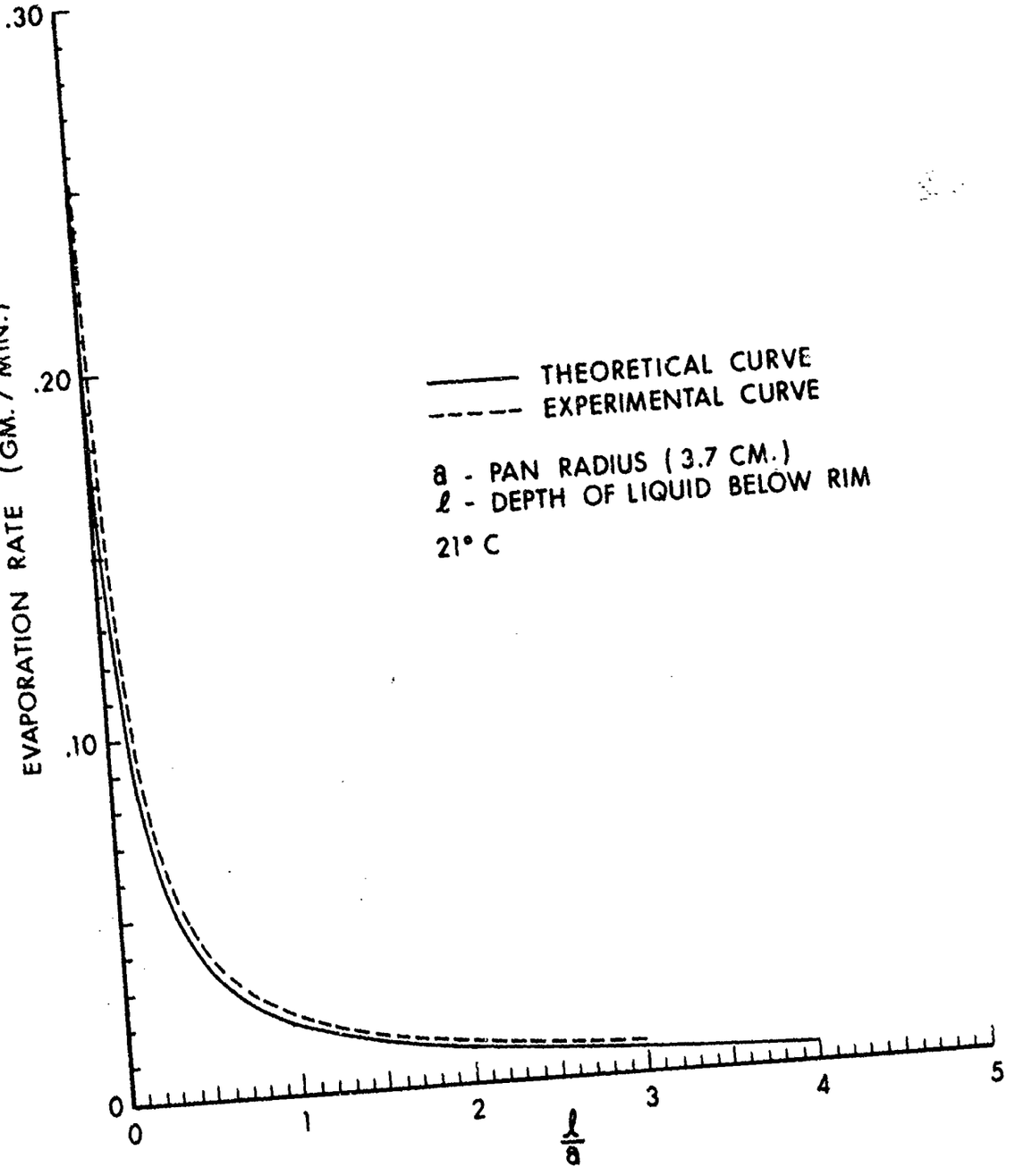

Figure 8. Evaporation Rate for Cyclohexane.

VII. BINARY MIXTURES OF ORGANIC LIQUIDS

The mass evaporation rate for a mixture of two liquids can be written as follows

$$\dot{m}_v = \frac{4\{1 + K'\beta (Re_1)^{1/2} (Sc_1)^{1/3}\}}{1 + \frac{4}{\pi}\{1 + K'\beta (Re_1)^{1/2} (Sc_1)^{1/3}\}\ell/a} \cdot \frac{P_{Fo_1}}{P_A} \cdot \frac{M_{F_1} P_A}{RT} \cdot D_1 \cdot a \cdot \gamma_1 \cdot x_1$$

(50)

$$+ \frac{4\{1 + K'\beta (Re_2)^{1/2} (Sc_2)^{1/3}\}}{1 + \frac{4}{\pi}\{1 + K'\beta (Re_2)^{1/2} (Sc_2)^{1/3}\}\ell/a} \cdot \frac{P_{Fo_2}}{P_A} \cdot \frac{M_{F_2} P_A}{RT} \cdot D_2 \cdot a \cdot \gamma_2 \cdot x_2.$$

Here it is assumed that the terms $\frac{P_{Fo_1}}{P_A} \cdot \gamma_1 \cdot x_1$ and $\frac{P_{Fo_2}}{P_A} \cdot \gamma_2 \cdot x_2$ are relatively small ($< \sim .2$). The evaporation rate is essentially a sum of the rates of the individual constituents of the mix with provision made for the non-ideal behavior of the mix through inclusion of the activity coefficients (γ's). The x's are the liquid mole fractions. The liquid is assumed to be thoroughly mixed.

Because of the possible non-ideal behavior of the mix (Raoult's law not obeyed) it is possible for a mixture of two liquids to evaporate faster than either of its two constituents. This fact can be demonstrated using the above equation and the fact that the activity coefficients may be greater than unity for certain mixtures. Such a non-ideal mixture is formed by cyclohexane and ethanol, and experimental results demonstrating that the mixture evaporates more rapidly than cyclohexane (the more rapidly evaporating component) are shown in Figure 9.

A computer program has been written for the HP 9810A computer to calculate mass evaporation rate as a function of time for binary mixtures. Other quantities of interest such as average liquid molecular weight, ℓ/a, liquid mole fractions, and liquid volume can be printed out as a function of time also. Quantities assumed constant are the liquid surface temperature, viscosity, and the average diffusion

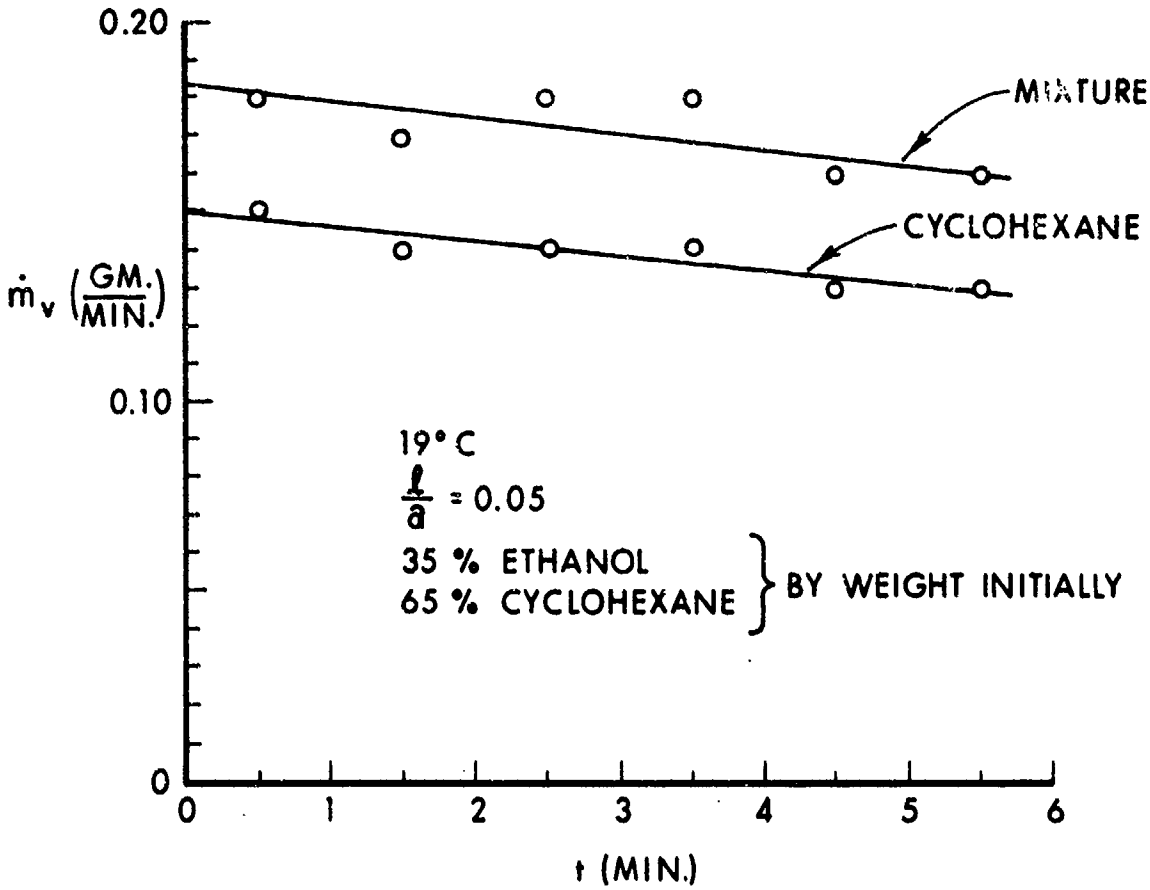

Figure 9. Mass Evaporation Rate of the Binary Azeotropic Mixture, Cyclohexane plus Ethanol.

coefficient. These are not bad assumptions for the cases considered so far. The liquid is assumed to be well stirred which is probably a good assumption for thin liquid layers. The code predicts that thin layers of mixtures lose their volatiles faster than thicker layers.

A mixture of one-third pentane and two-thirds octane by volume was considered as a trial case for the program. Twelve milliliters of liquid were placed in a pan 3.7 cm in radius and 0.57 cm deep. The experimental results are shown in Figure 10 together with the theoretical curve for comparison. Note that the theory gives excellent agreement over a range from one to two minutes up to ten minutes or perhaps longer. In the early stages the experimental data is thought to be higher because the liquid surface temperature is slightly higher than the median value stated. Also a short time is required to achieve pseudo-steady state vapor concentration profiles leading to a higher initial rate.

Binary mixtures can be used to approximate the vaporization characteristics of common vehicle fuels. Figure 10 shows how closely the one-third pentane two-thirds octane mixture approximates a sample of combat gasoline vaporizing from an open pan. Agreement is seen to be quite good from three to ten minutes and probably longer. Addition of another less volatile component would be expected to extend the agreement to very long times. Addition of a more volatile component would be expected to improve agreement at short times.

VIII. FLAMMABLE SURFACES DEVELOPMENT FOR PURE LIQUIDS, MIXTURES AND FUELS

The time development and extent of the flammable volume over a fuel spill are important input for the military fuel fire problem.

The steady state flammable volume over a vaporizing pure hydrocarbon (hexane) in a circular pan is shown in Figure 7 [$\ell/a \approx 0.08$]. The experimentally determined surface shown in the figure represents the lower flammable limit (LFL) concentration of vapor in air. The upper flammable limit (UFL) concentration is much closer to the liquid surface. The horizontal extent of the flammable volume depends critically on ℓ/a for

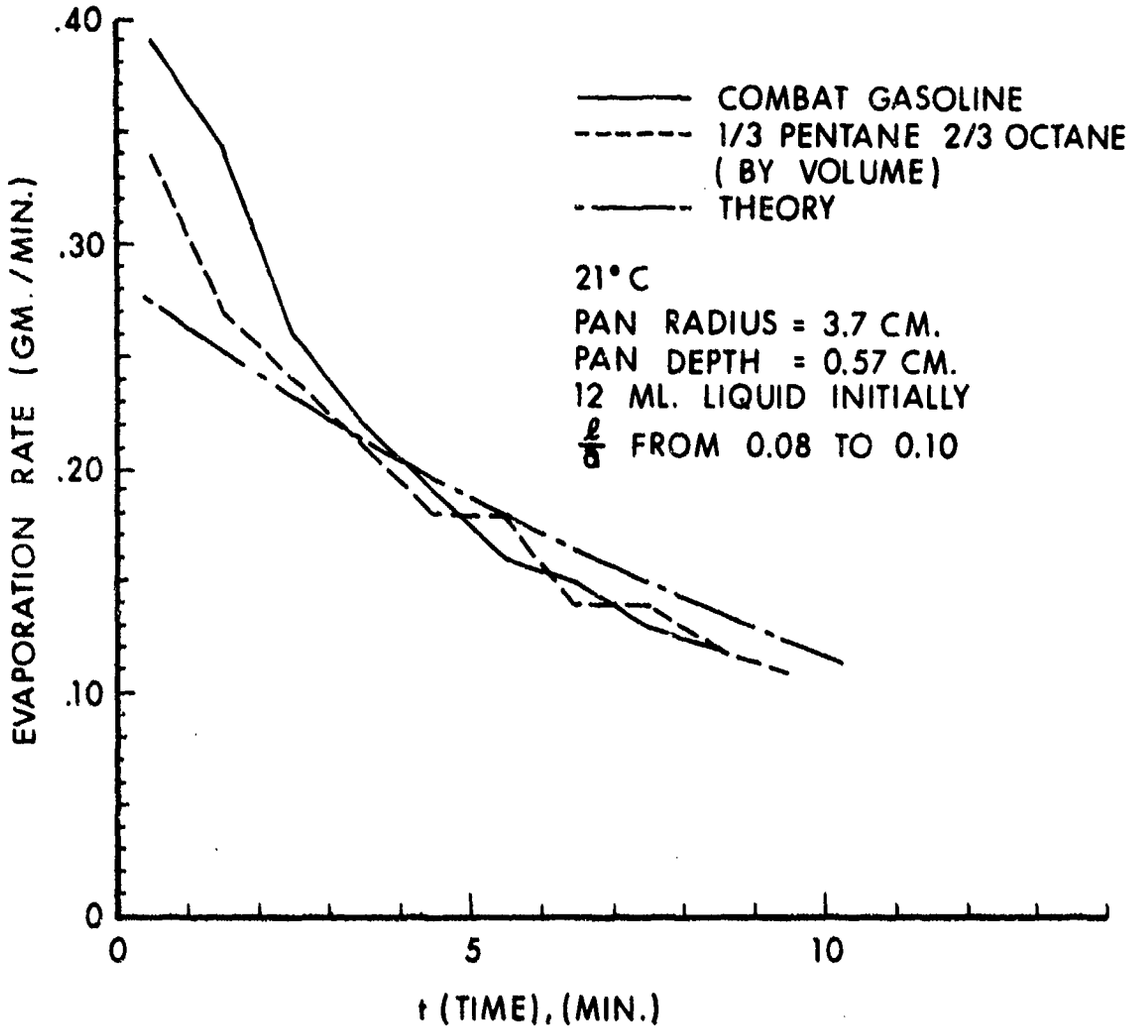

Figure 10. Evaporation Rates, Combat Gasoline and 1/3 Pentane - 2/3 Octane Mixture.

small ℓ/a. A large box surrounds the pan and limits the influence of external air currents on the system. The air motion in the box is random with an average air speed of some 2 - 3 cm/sec (DISA and TSI low velocity anemometers employed, velocity slightly lower than in the laboratory room).

Slight changes in time, of the velocity distribution representing the air motion in the vicinity of the pan, imply that the flammable envelope will fluctuate with time. The average flow direction and magnitude vary slightly with time to produce small changes in the extent of the envelope. Measurements show that the hexane envelope has a radial uncertainty in the plane of the pan of ± 1 cm for vaporization from the 3.7 cm pan under the flow conditions in the box. As the flow velocity is increased in one direction parallel to the liquid surface the flammable envelope becomes increasingly elliptical in shape as viewed from above. A capacitance spark probe is used to locate the flammable limit surfaces. The entire apparatus is shown in Figure 11. The spark energy (several hundred mj) is much above the minimum ignition energy for the particular electrode spacing (~ 1 mm) employed, according to the criteria of Lewis and von Elbe as discussed in Mullins and Penner[15].

The experimentally determined vertical height of the LFL surface for hexane over a 3.7 cm radius pan is approximately 1.0 cm (for ℓ/a ≈ 0). Three-dimensional diffusion theory (Section V) would predict a much higher value, on the order of 30 cm., showing the inadequacy of a pure diffusion approach at this relatively large pan size. However, for smaller pan size pure diffusion effects become more important due to increasing per unit area vapor flux at the liquid surface (see combined rate expression for small Re). For the 3.7 cm and larger pans an approximate rule has been developed for predicting the maximum height of the LFL surface. For these pan sizes the flow velocity in the box is dominant in determining the vertical height of the LFL surface. It has been found that the vertical height predicted from the 2D boundary layer flow theory at a distance 'a' (one pan radius) from the leading edge agrees approximately with the measured heights at the center of

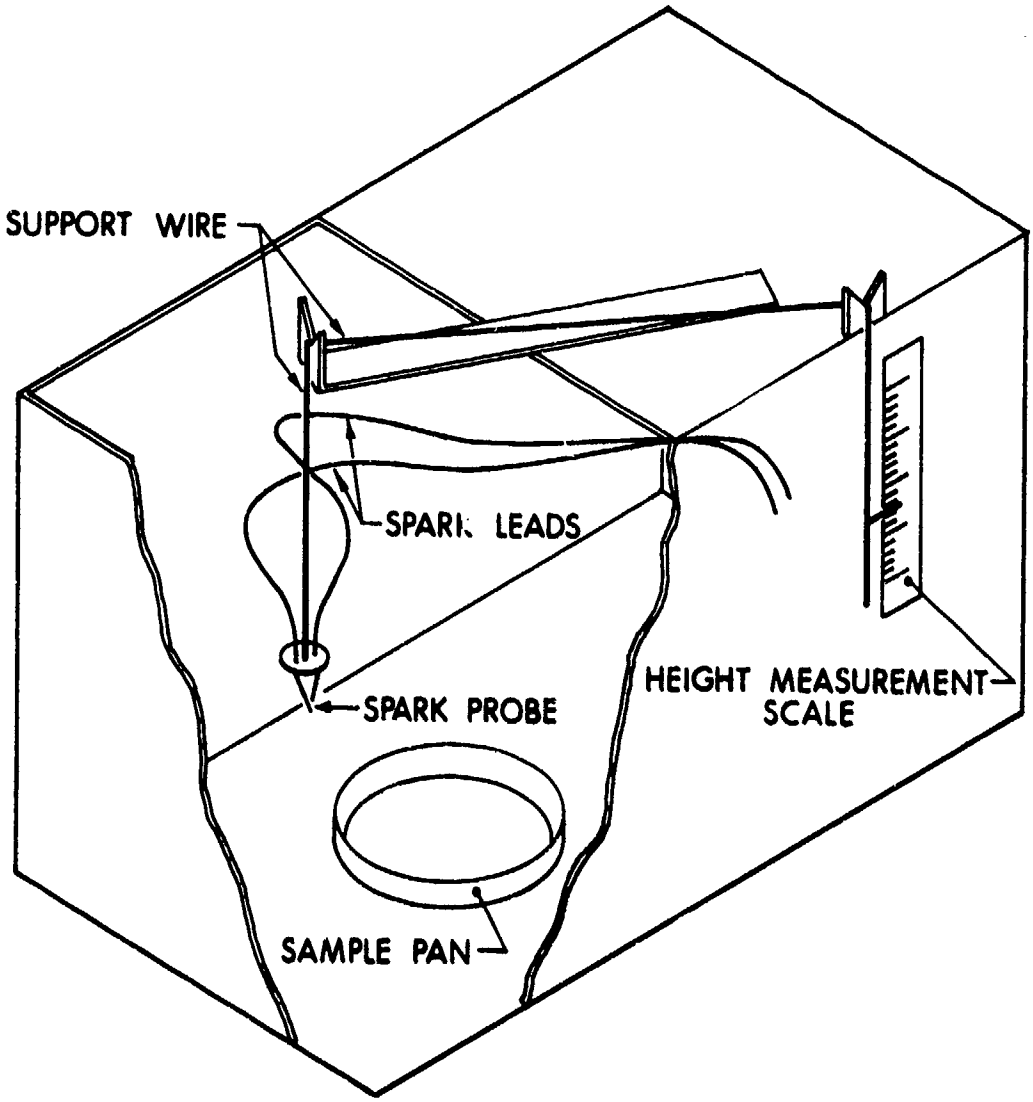

Figure 11. Apparatus for Flammable Surface Study.

the 3.7 cm and larger radii pans. For example, for the 3.7 cm pan the computed height (using the LFL concentration) is about 1.1 cm which agrees with the measurement (assuming a 3 cm/sec flow). The 2D theory predicts an $a^{1/2}$ power dependence for the vertical height which is approximately what is observed as one goes to larger pan sizes. This same calculation appears to work for the UFL surface also, but experimental data is not complete.

The 2D theoretical results are presented by Bird, Stewart, and Lightfoot[7]. Computations of flammable heights based on these results depend on the evaluation of the incomplete gamma function. An interesting relationship between the incomplete gamma function and the confluent hypergeometric function exists which permits an accurate evaluation of the gamma function. The hypergeometric function is tabulated in the NBS Handbook of Mathematical Functions. The relationship is as follows

$$\frac{\Gamma\left(\frac{1}{3}, u\right)}{\Gamma\left(\frac{1}{3}, \infty\right)} = \left\{\frac{M\left(1, \frac{1}{3}, u\right) - 1}{u}\right\} \frac{u^{1/3}\, e^{-u}}{2.68} \tag{51}$$

where $\Gamma\left(\frac{1}{3}, u\right)$ is the incomplete Γ function according to Bird and $\Gamma\left(\frac{1}{3}, \infty\right)$ is the complete Γ function ($= 2.68$). $M\left(1, \frac{1}{3}, u\right)$ is the confluent hypergeometric function. The incomplete Γ function is related to the mole fraction vapor concentration by

$$\frac{\Gamma\left(\frac{1}{3}, u\right)}{\Gamma\left(\frac{1}{3}, \infty\right)} = 1 - \frac{x_F}{x_{Fo}} \tag{52}$$

where x_F is the vapor mole fraction at η, and x_{Fo} is the mole fraction at the liquid surface. Also

$$u = \frac{1.328}{3!} \cdot A_{FA} \cdot \eta^3 \tag{53}$$

$A_{FA} = \frac{\nu}{D}$ $\quad$ ν kinematic viscosity
$\quad$ $\quad$ D binary diffusion coefficient

and

$$\eta = \frac{y}{2}\sqrt{\frac{u_\infty}{\nu x}}$$

'y' is the height above the liquid surface at distance 'x' from the leading edge ('x' taken to be equal to 'a' in this case). u_∞ is ~ 3 cm/sec, the average air speed.

Note the great horizontal spread of the experimentally determined LFL surface (Figure 7) extending some 7 cm beyond the pan rim (3.7 cm radius pan, $\ell/a \approx 0.08$, for hexane). No mathematical theory is presented to describe this phenomenon but it is felt to be due to the high molecular weight of the hexane vapor which causes it to fall close to the base plate after it clears the pan rim. Only liquids of relatively high evaporation rate (and proper flammable limit) exhibit this large horizontal spread.

Thus far discussion has been limited to the steady state surface. Time development of the LFL surface of hexane is shown in Figure 12. The time development study was confined to a study of the horizontal development of the surface (in the plane of the pan) as this was easiest to measure ($\ell/a \approx 0.08$ in Figure 12). Note that the flammable region develops rapidly at first and then more slowly with steady state reached in some five to ten minutes at ~ 7 cm. Two types of initial conditions were employed. In one the liquid was poured into the pan (5 seconds required to pour) and time zero was taken at the end of the pour. In the other the liquid was poured into the container then covered quickly with a glass plate. The glass plate was then removed to begin the test (time zero). Both methods gave closely similar results.

Mixtures and fuels showed interesting flammable surface development. Results (again in the plane of the pan) are shown for a 1/3 pentane - 2/3 octane mixture (by volume) and for a sample of combat gasoline in Figure 13. The results obtained for the (again $\ell/a \approx 0.08$) binary mixture and for the gasoline are indistinguishable over a period of 10 minutes. Note the development, an initial rapid increase occurs followed by a more gentle rise with a maximum reached in some two or

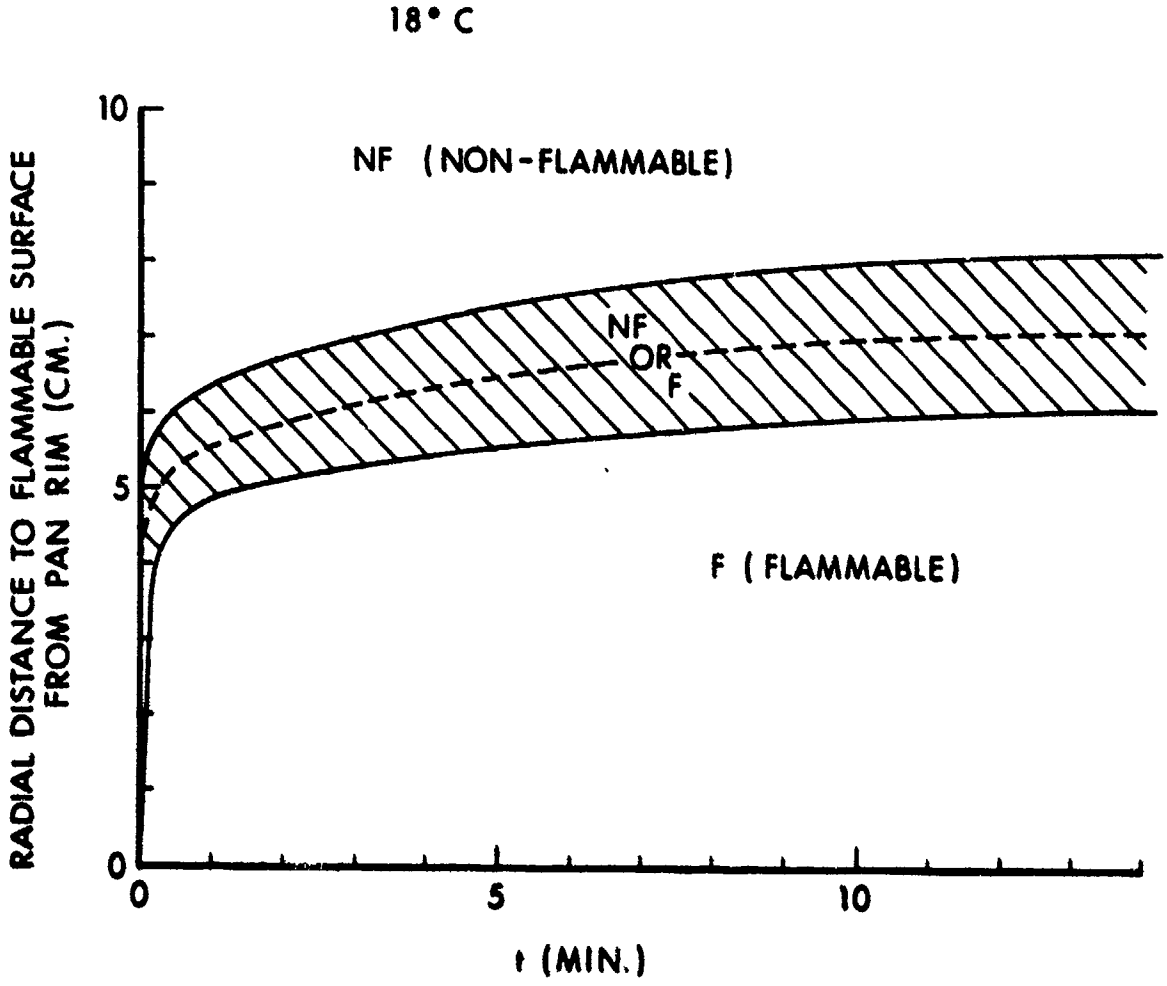

Figure 12. Time Development of the Flammable Surface of Hexane (In the Plane of the Liquid Surface).

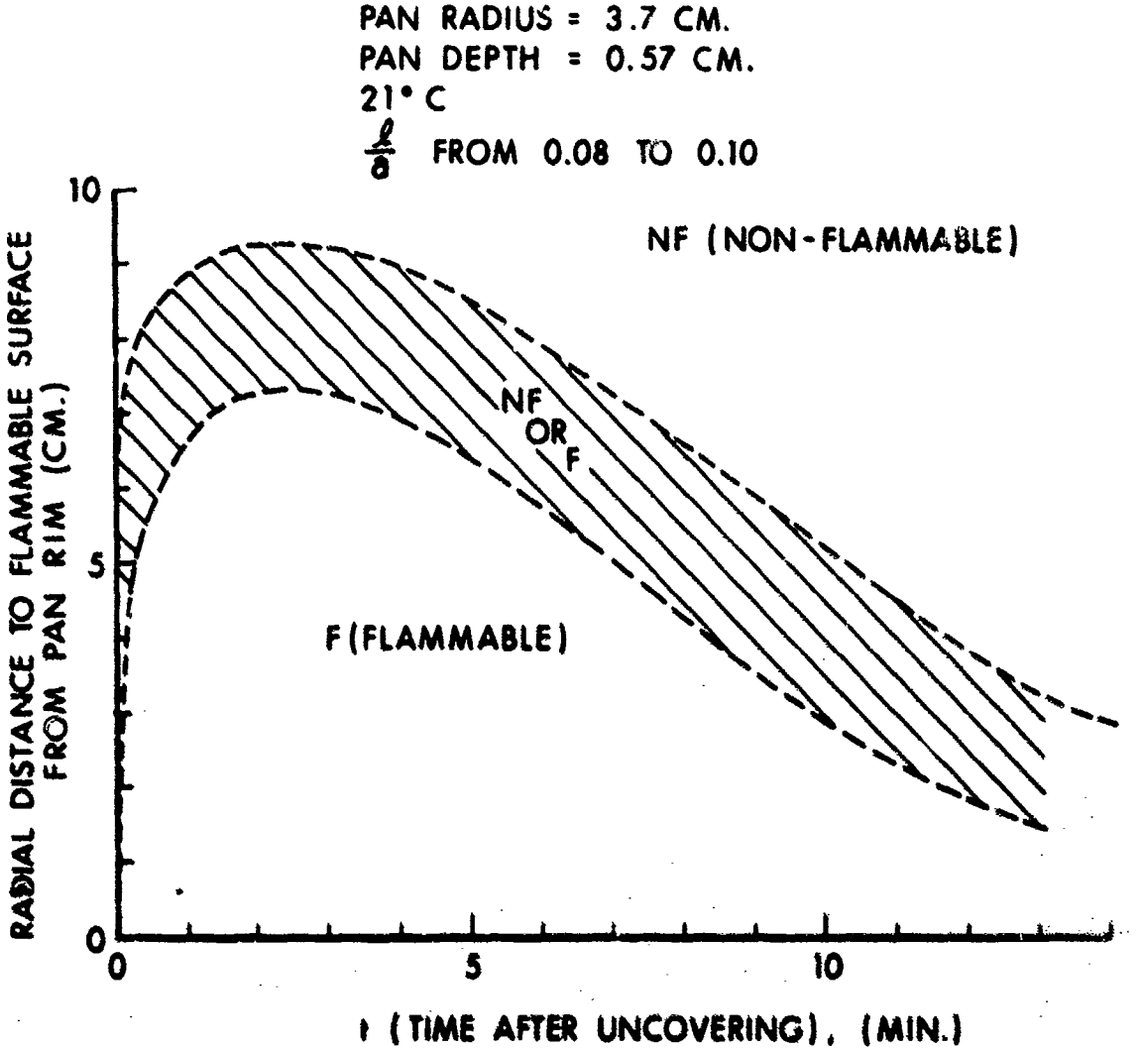

Figure 13. Flammable Surface Development for a Typical Sample of Combat Gasoline and for a Mixture of 1/3 Pentane-2/3 Octane.

three minutes (at 8 or 9 cm. for the LFL surface). Then the surface starts to shrink as the loss of volatiles begins to dominate. A thin layer of gasoline allowed to sit in an open space for some fifteen minutes is a good bit safer than a freshly poured sample.

IX. EVAPORATION RATES FOR PURE LIQUIDS WITH UNKNOWN SURFACE TEMPERATURE (THE HEAT TRANSFER PROBLEM)

The theoretical evaporation rate expression developed in Section VI for pure liquids dopended on a knowledge of the surface temperature of the evaporating liquid. If the liquid surface temperature is unknown the problem becomes much more complicated since the heat transfer characteristics of the system must also be evaluated.

Figure 14 depicts the energy balance in pseudo-steady state vaporization. In the near steady state the heat liberated by the liquid surface ($\dot{Q}_v$) due to evaporation is balanced by the heat supplied by conduction and convection through the base, liquid, and air $[(-K_H)(T - T_A)]$. $\dot{Q}_v$ is obtained by multiplying $\dot{m}_v$ (the mass evaporation flux, see Section VI) by the heat of vaporization L. K_H is the heat transfer coefficient of the air, liquid and base. In the near steady state the liquid surface will be at some temperature (T_s) less than the ambient temperature (T_A).

The evaporative heat flux curves for two liquids are shown in Figure 14. The liquid with the lower evaporative heat flux $\dot{Q}_{v_2}$ (less than $\dot{Q}_{v_1}$) has a surface temperature (T_{s_2}) closer to ambient other factors being equal. The implication is that either the mass evaporation rate or the heat of vaporization or both are less for liquid two. Simple qualitative experiments easily demonstrate these effects.

The heat transfer coefficient (K_H) can be altered by changing the base material or viscosity of the liquid (by adding a thickener) or both. An aluminum or lead base plate gives a high surface temperature (T_{s_1} for liquid 1), a glass base gives a lower temperature, and a wood or paper base gives a still lower temperature (T'_{s_1} for liquid 1).

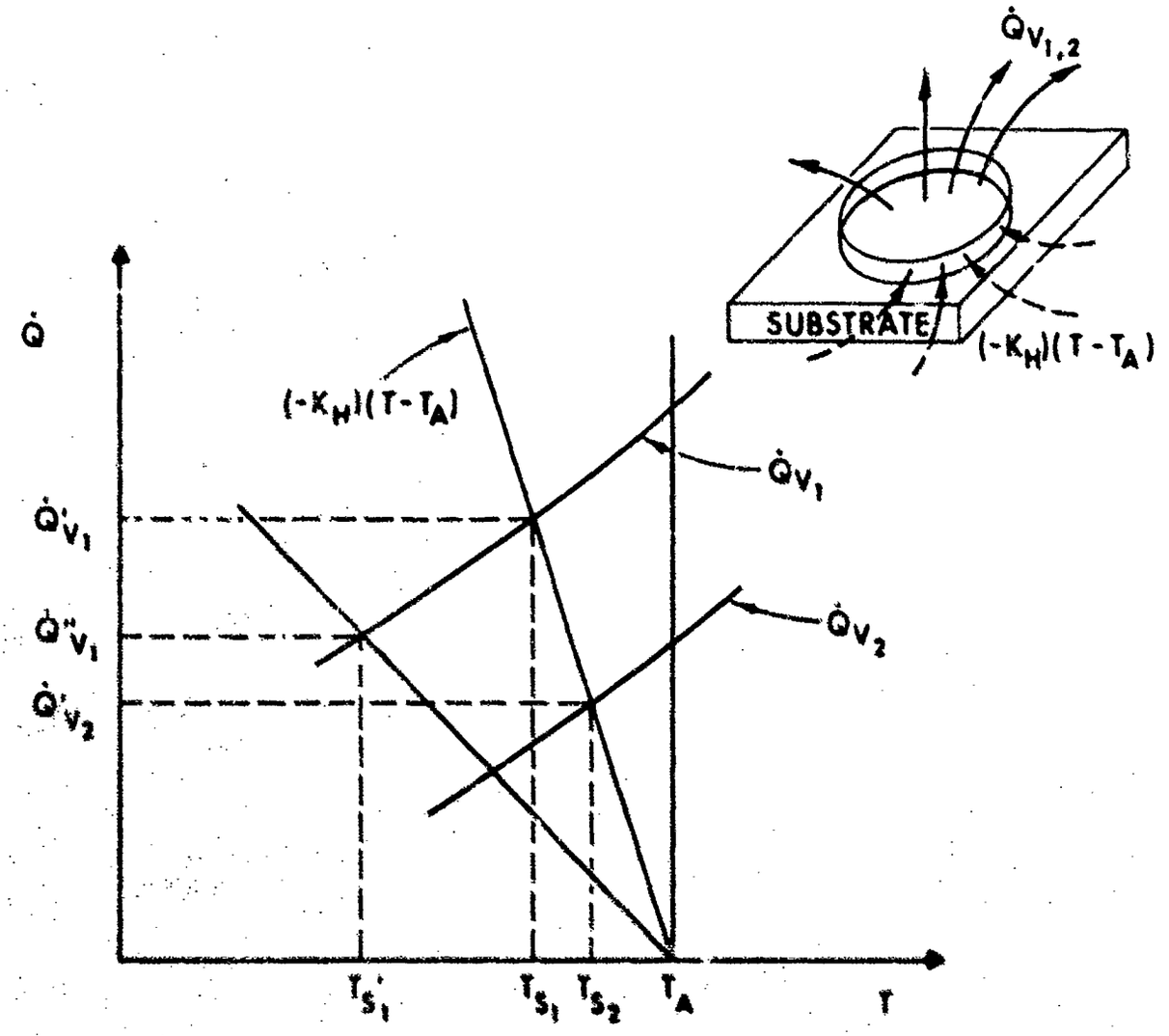

$\dot{Q}$ - HEAT FLUX

T - TEMPERATURE

$\dot{Q}_{V_{1,2}} = \dot{m}_{V_{1,2}} \cdot L_{1,2}$

$L_{1,2}$ - HEAT OF VAPORIZATION OF LIQUID 1 OR 2.

T_S - SURFACE TEMPERATURE

T_A - AMBIENT TEMPERATURE

K_H - AIR-LIQUID-BASE HEAT TRANSFER COEFFICIENT

Figure 14. Effect of Substrate on Vaporization.

The temperature effects are most pronounced for liquids with high heat flux rates (like $\dot{Q}_{V_1}$ in the figure). Increasing the viscosity of a liquid by adding a thickener decreases the heat transferred through it. An evaporating liquid is in constant motion[16] and transfers a significant amount of heat by convection. A thickener was added to cyclohexane to restrict the motion. The result as expected was a reduction in the surface temperature with a consequent reduction in evaporation rate (on aluminum base plate).

X. EVAPORATION MEASUREMENTS WITH THE TGA

The thermogravimetric analyzer (Dupont Model 950) is a very useful instrument for making rapid determinations of relative evaporation rates. Fairly reliable measurements can be made in a period of a few minutes whereas other methods require considerably longer. The TGA test tube section is shown in Figure 15. The test liquid whose evaporation rate is to be measured is placed in the boat. Dry N_2 gas is passed over the liquid parallel to the surface (a glass ball flow meter is used to monitor the N_2 from a gas bottle). The boat is partially entered into the furnace, the degree of entry is adjusted until the liquid surface temperature (as measured by the thermocouple which is placed close to the liquid surface) is steady at 20°C. The temperature is monitored at intervals throughout the test. The volatility and heat of vaporization of the liquids determine how far the boat must be pushed into the furnace. The evaporation rate is measured after steady state temperature is reached by taking the slope of the mass loss time curve as recorded on the TGA chart recorder.

The evaporation rates measured with the TGA correlate approximately with the product of the diffusion coefficient (D), molecular weight (M_v), and vapor pressure (P_{Fo}) (Figure 16). The TGA evaporation rate is equally divided between pure diffusion and flow controlled evaporation. For flow controlled evaporation the correlation would involve $D^{2/3}$ (in place of D), such a correlation is also good in this case. Uncertainties in the TGA data are due to uncertainties in surface temperature, in

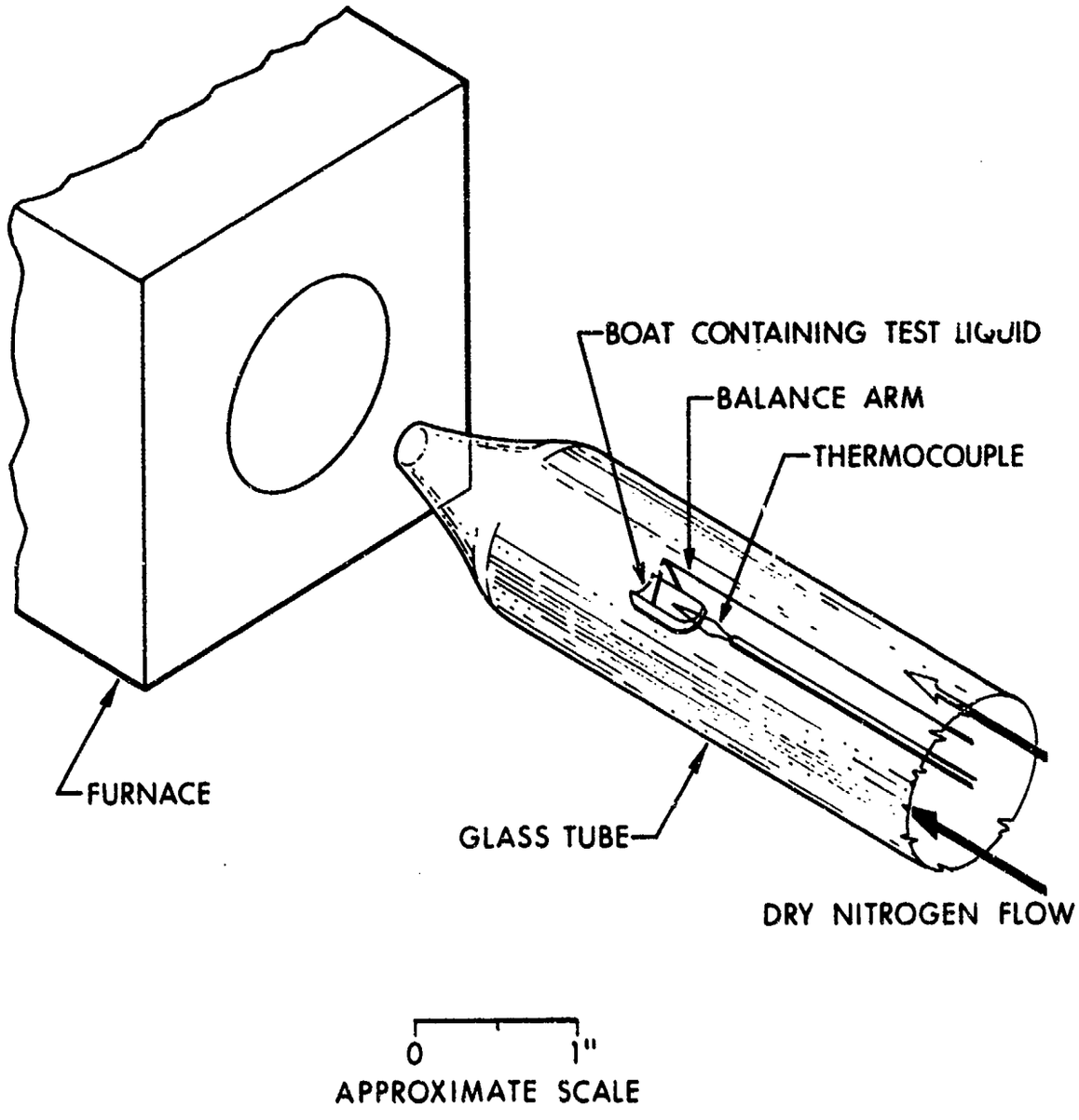

Figure 15. Thermogravimetric Analyzer.

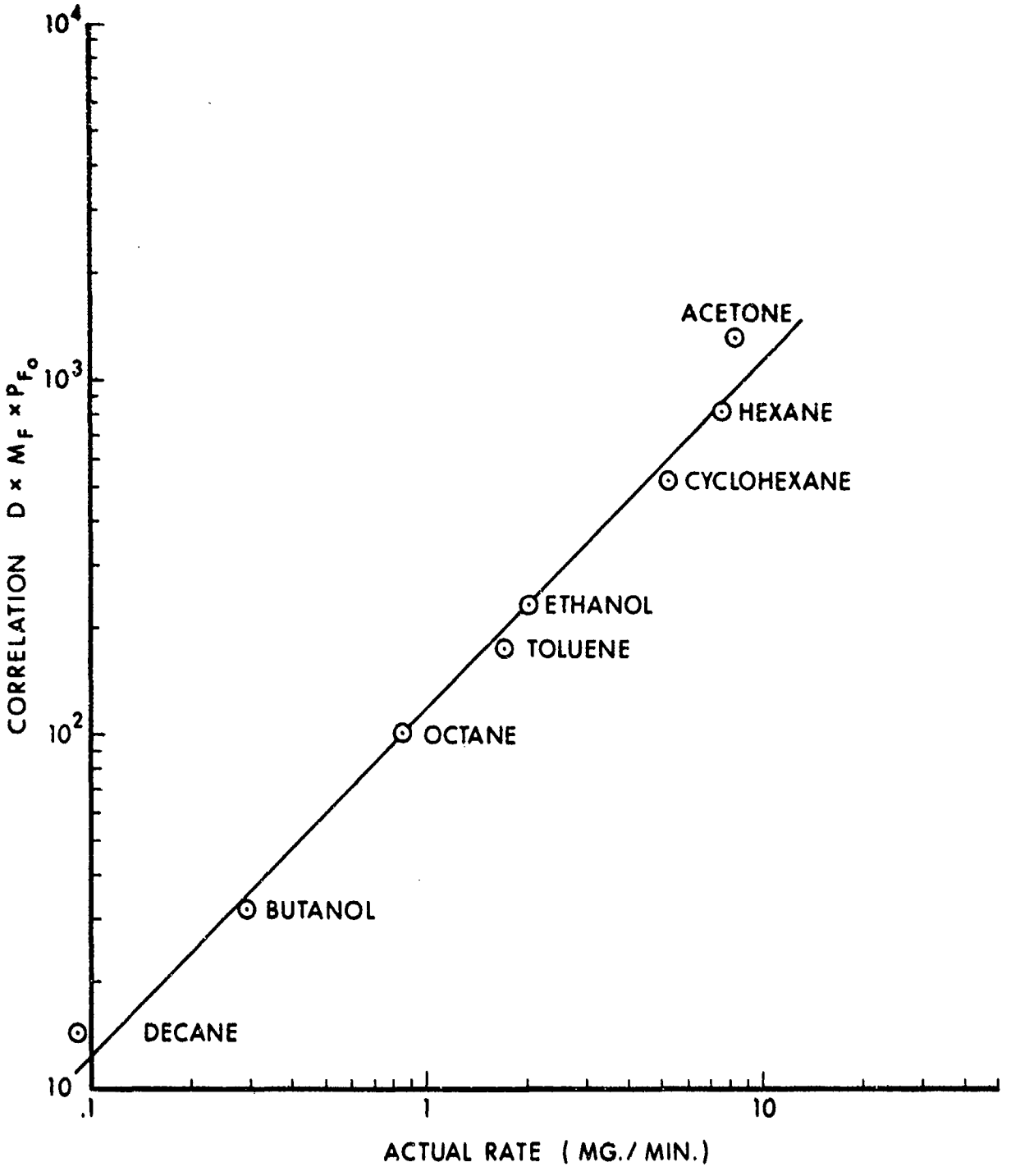

Figure 16. Evaporation Rate Correlation Determined from DuPont 950 Thermogravimetric Analyzer.

diffusion coefficient, and in pan orientation. The change in depth of the liquid below the boat rim during the course of a run is not sufficient to cause more than a ± 10% variation in the evaporation rate. Evaporation rate measurements were made with the boat between two-thirds and one-third full.

XI. CONCLUSIONS

Even very slow air movement (on the order of a few cm/sec.), such as might be encountered in a laboratory room, significantly affects the vaporization rate and flammable envelope of a pool of liquid hydrocarbon. The effects of such small air currents on evaporation from pools have not been generally recognized much less quantified up to this time. The mass evaporation rate expression developed in Section VI has been shown to effectively model evaporation into slow moving air where the velocity distribution is reproducible over the period of the evaporation rate measurements. The expression successfully predicts rates from decane in the smallest pan (2 cm. diameter) to acetone in the largest pan (17 cm. diameter), a factor of one thousand in evaporation rate. The evaporation rate of six other liquids intermediate between decane and acetone are also correctly predicted. The expression used here has general applicability for many types of evaporation problems.

Vaporization rates of fuels are quite time dependent since fuels are composed of many different hydrocarbons. The vaporization characteristics of common vehicle fuels have been approximated here at BRL by simple mixtures of pure hydrocarbons. Even a binary mixture can do an effective job over a moderate length of time as has been demonstrated in the laboratory. A particular sample of regular combat gasoline has been effectively modeled over a period of at least ten minutes by a mixture of 1/3 pentane - 2/3 octane (by volume). The great advantage of using a binary mixture is that accurate theoretical predictions of its vaporization rate (and hence that of the fuel) can be made using the computer program described in Section VII. This program could be extended to treat n-component mixtures and hence do a more effective job

at approximating a fuel.

The flammable region associated with a spill of liquid fuel or any combustible liquid above its flash point is not limited to the physical size of the spill but extends appreciably beyond and above the spill where the vapor-air mixture is flammable. Air motion is critical in determining the extent of the envelope. Detailed studies of the time development of the flammable envelope surrounding pools of various combustible liquids have been conducted here at BRL. For a pure liquid, such as hexane exposed to slow moving air (see Figure 1), the flammable surface develops rapidly at first and then more slowly with steady state reached in approximately five minutes after the pool is initially exposed to the atmosphere. The vertical height of the steady state surface is proportional to the square root of the pan radius and is relatively small compared to the horizontal extent of the surface. For a mixture of hydrocarbons such as gasoline the flammable envelope expands at first, as with hexane, but then dramatically collapses as the more volatile components are lost. Thus a pool of gasoline exposed to the open air is relatively safer after a prolonged length of time than it is in the first few minutes. The binary mixture 1/3 pentane - 2/3 octane shows a flammable envelope which develops in nearly identical fashion to the sample of combat gasoline. Knowing the appropriate binary mixture enables one to calculate the height of the flammable envelope as a function of time. Results such as these show how very useful mixtures can be in approximating fuels.

In conclusion then, advances have been made in the theoretical description of liquid pool evaporation and in the theoretical and experimental analysis of flammable envelope development. Also considerable success has been achieved in the use of a simple mixture to model a real fuel.

REFERENCES

1. Wyllie, G., "Evaporation and Surface Structure of Liquids," Proc. Roy. Soc., (London) A197 pp. 383-395 (1949).

2. Heideger, W. J., and Boudart, M., "Interfacial Resistance to Evaporation," Chemical Engineering Science, Vol. 17, pp. 1-10 (1962).

3. Schrage, R. W., A Theoretical Study of Interphase Mass Transfer, Columbia University Press, New York (1953).

4. Lee, C. Y., and Wilke, C. R., "Measurement of Vapor Diffusion Coefficient," Industrial and Engineering Chemistry, Vol. 46, No. 11, pp. 2381 - 2387 (1954).

5. Altshuller, A. P., and Cohen, I. R.,"Application of Diffusion Cells to the Production of Known Concentrations of Gaseous Hydrocarbons," Analytical Chemistry, Vol. 32, No. 7, pp. 802 - 810 (June 1960).

6. Heinzelmann, F. J., Wasan, D. T., and Wilke, C. R., "Concentration Profiles in a Stefan Diffusion Tube," I. & E. C. Fundamentals, Vol. 4, No. 1, pp. 55 - 61 (Feb. 1965).

7. Bird, R. B., Stewart, W. E., Lightfoot, E. N., Transport Phenomena, John Wiley and Sons Inc., New York, pp. 594 - 598, 615 - 616 (1960).

8. Danckwerts, P. V., "Unsteady-State Diffusion or Heat-Conduction with Moving Boundary," Trans. Faraday Soc., Vol. 46, pp. 701 - 712 (1950).

9. Fuchs, N. A., Evaporation and Droplet Growth in Gaseous Media, Itogi, No. 1, All-Union Institute of Scientific Technical Information, Academy of Sciences (U.S.S.R.), pp. 4 - 5, 44 (1958).

10. Vaillant, M. P., "A Special Case of Evaporation," Compt. rend., Vol. 150, pp. 689 - 691 (March 1910).

11. Tarifa, C. S., Notario, P. P., Valdes, E. C., "Open Fires," U. S. Department of Agriculture Forest Service, Final Report of Grants FG-SP-114 and FG-SP-146 (Vol. 1), Madrid (May 1967).

12. Rosenhead, L., Laminar Boundary Layers, Oxford University Press, pp. 222 - 226 (1963).

13. "The Present State of the Hydrodynamics of Viscous Liquids," (Sovremennoye sostoianiye gidrozerodinamiki viazhoi zhidkosti), I. L., M, 2, pp 265 (1948).

14. Thomas, N., Ferguson, A., "On Evaporation from a Circular Water Surface," Philosophical Magazine, Vol. 34, pp 309, 316 - 321 (1917).

15. Mullins, B. P., Penner, S. S., Explosions, Detonations, Flammability and Ignition, Pergamon Press, New York, Chapt. XIII, (1959).

16. Spangenberg, W. G., Rowland, W. R., "Convective Circulation in Water Induced by Evaporative Cooling," The Physics of Fluids, Vol. 4, No. 6, pp 743 - 750 (June 1961).